8-1-1989

Propagation of Nonsinusoidal Waveforms in Power Systems

Robert Sparks
Purdue University

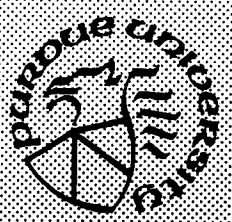

Propagation of Nonsinusoidal Waveforms in Power Systems

Robert Sparks

TR-EE 89-37
August, 1989

School of Electrical Engineering
Purdue University
West Lafayette, Indiana 47907

this is dedicated
to my mom and dad

ACKNOWLEDGMENTS

I would like to thank Professor Heydt for the initial idea and motivation to do this research and for his valuable input throughout the process. I would like to thank Professor Ogborn and Professor Ong for reviewing this thesis. I would also, like to thank Mary Schultz for typing this thesis.

LIST OF TABLES

Table Page

3.1 Alternative choices of sampling parameters 37

TABLE OF CONTENTS

Page

LIST OF TABLES vi

LIST OF FIGURES vii

ABSTRACT ix

CHAPTER 1 - INTRODUCTION 1

1.1 Motivation 1

1.2 Literature Summary of Some Transforms and Transform Properties Used In Circuit Analysis 2

1.3 Literature Summary of Some Methods for Calculating the Propagation of Non-Sinusoidal Waveforms in Power Systems 7

1.4 Organization of This Thesis 9

CHAPTER II - PROBLEM FORMULATION AND SOLUTION 11

2.1 Calculation of Transfer Impedances 11

2.2 Laplace Transform Method 12

2.3 Fourier Transform Method 13

2.4 Hartley Transform Method 17

CHAPTER III - DEMONSTRATION OF THE FREQUENCY DOMAIN METHODS 18

3.1 The Example System 18

3.2 Laplace Transform Solution 20

Page

3.3 Fourier Transform Solution 20

3.4 Hartley Transform Solution 26

3.5 Choice of Sampling Parameters 26

CHAPTER IV - POWER SYSTEM REPRESENTATION 38

4.1 Modeling of the Network Components 38

4.2 Sensitivity of Circuit Solution to Model Parameters and Injection Current Characteristics 39

CHAPTER V - CONCLUSIONS AND RECOMMENDATIONS 53

LIST OF REFERENCES 55

APPENDIX 58

LIST OF FIGURES

Figure Page

2.1 Block diagram of the Fourier transform method 15

2.2 Illustration of the errors introduced by the Fourier transform method 16

3.1 The example power system 19

3.2 The nonsinusoidal current injected into bus 8 21

3.3 Laplace transform solution of the voltage at bus 1 22

3.4 SPICE solution of the voltage at bus 1 23

3.5 Fourier transform solution of steady state voltage at bus 1 24

3.6 SPICE solution of steady state voltage at bus 1 25

3.7 Fourier transform zero initial state solution at bus 1. Found by zero packing the current waveform samples after 0.0167 seconds 27

3.8 Fourier transform zero initial state solution at bus 1. The first 0.0167 seconds of Figure 3.7 28

3.9 Injection current with a rise proportional to t^3. This current will be used in studies from this point on. This current is injected into bus 8 29

3.10 Fourier transform solution of steady state voltage at bus 1 due to current in Figure 3.9 30

3.11 Fourier transform solution of steady state voltage at bus 8 to current in Figure 3.9 31

3.12 Hartley transform representation of frequency spectrum of transfer impedance $Z_{1,8}$ 32

Figure Page

3.13 Magnitude of Fourier transform representation of frequency spectrum of transfer impedance $Z_{1,8}$. Resonant frequency is at 4900 rad/sec 33

3.14 Phase of Fourier transform representation of transfer impedance $Z_{1,8}$ ..34

3.15 Magnitude of frequency spectrum of current shown in Figure 3.9, Fourier representation 36

4.1 Injection current with high frequency characteristics due to short duration of pulses, injected into bus 8 40

4.2 Voltage response at bus 1 due to pulse current in Figure 4.1.....41

4.3 Magnitude of frequency spectrum of pulse current in Figure 4.1 42

4.4 Magnitude of frequency spectrum of transfer impedance $Z_{1,8}$. All transmission line impedances have been increased to 0.01 + j 0.1 (pu). Resonant frequency is at 4523 rad/sec.....45

4.5 Voltage at bus 1 due to current in Figure 3.9. All transmission line impedances have been increased to 0.01 + j 0.1 (pu).....46

4.6 Magnitude of frequency spectrum of transfer impedance $Z_{1,8}$. Transformer series impedance has been changed to 0.005 + j 0.05 (pu). Resonant frequency is at 6974 rad/sec.....47

4.7 Voltage at bus 1 due to current in Figure 3.9. Transformer series impedance has been changed to 0.005 + j 0.05 (pu) 48

4.8 Magnitude of frequency spectrum of transfer impedance $Z_{1,8}$. External system equivalent impedance has been changed to 0.01 + j 0.01 (pu). Resonant frequency is at 4712 rad/sec.....49

4.9 Voltage at bus 1 due to current in Figure 3.9. External system impedance has been changed to 0.01 + j 0.01 (pu).....50

4.10 Magnitude of frequency spectrum of transfer impedance $Z_{1,8}$. All shunt capacitances have been increased by a factor of 10. Resonant frequency is at 1696 rad/sec 51

4.11 Voltage at bus 1 due to current in Figure 3.9. All shunt capacitances have been increased by a factor of 10.....52

ABSTRACT

Sparks, Robert. M.S.E.E., Purdue University. August 1989. Propagation of Nonsinusoidal Waveforms in Power Systems. Major Professor: G. T. Heydt.

Several computationally efficient and innovative methods for the calculation of power system voltages due to nonsinusoidal demand currents are studied. The method is useful for power quality calculations. The method is introduced by using Laplace transform analysis to simplify the convolution of the transfer impedances and the demand currents. An iterative numerical inverse Laplace transform method is briefly examined. However, the problem characteristics allow Fourier transform analysis to be used. Furthermore, the fast Fourier transform is used to approximate the continuous Fourier transform. This discrete transform analysis method proves to be conveniently suitable to the problem definition. More importantly the discrete transform method proves to be superior to well known time domain methods. A real transform, the Hartley transform, which is computationally more efficient than the complex Fourier transform is also used to solve the problem. The methods are tested on an eight bus example power system. The main contribution of this thesis is the presentation of computationally efficient methodologies which are useful for the accurate analysis of the propagation of nonsinusoidal waveforms in power systems.

CHAPTER I
INTRODUCTION

1.1 Motivation

The introduction of reliable and cost effective thyristors and other solid state power converters has caused an increase in the number of power system loads whose demand currents are nonsinusoidal. The presence of these nonsinusoidal currents in power systems causes distortion of the 60 Hz fundamental voltage and current waves. Many power system components are designed to operate with pure 60 Hz sinusoidal waveforms, and if this waveform is sufficiently distorted, the components may operate improperly or experience decreased life. Therefore, it is essential that the power system engineer be able to analyze how these nonsinusoidal currents propagate in a power system so that potential problems can be corrected.

Many of the waveforms produced by power electronic loads contain rapid decays and impulse-like characteristics. These phenomena usually result in high frequency components in the current spectrum. If the current switching occurs such that the resulting waveform is periodic, the frequency spectrum is discrete. If the current is nonperiodic, such waveforms generate a continuous frequency spectrum. In any case, the power system must be analyzed over a range of frequencies. In addition the power system contains transmission lines, transformers, and other components which contain frequency dependent parameters and nonlinearities. With these comments in mind, one quickly realizes that the analysis of nonsinusoidal waveforms in power systems is a nontrivial problem.

There are numerous techniques in circuit analysis which can be used to solve this problem. The problem could be solved in the time domain by writing the differential equations and numerically solving them. These methods have the advantage of convenience in modelling (especially nonlinearities). Also, there are several, well known numerical methods for digital implementation and solution. The main disadvantages of time solutions are long execution times, poor insight into the problem solution, and inconvenience in certain types of modelling (e.g., frequency dependent

parameters). Alternatively, the problem could be solved in the frequency domain. For linear circuits, the problem may be transformed to the frequency domain by the use of the Fourier transform or the Laplace transform. Then since the system can be modeled as a linear system, time convolution which is simple multiplication in the frequency domain can be used to solve the problem. Advantages of transform methodologies usually include high speed and potentially useful insight into the problem. Disadvantages often include inability to handle nonlinearities, and certain numerical problems relating to convergence.

The purpose of this research is to compare these different techniques. However, the emphasis of this work is on the formulation of frequency domain methods of solution which employ the use the fast Fourier transform. In addition, an alternative transform, the Hartley transform, is introduced and included in the comparison.

1.2 Literature Summary of Some Transforms and Transform Properties Used In Circuit Analysis

Fourier transform

Given f(t) a real or complex function of real variable t, the Fourier transform of f(t) is then [1]

$$\mathcal{F}\{f(t)\} = F(\omega) = \int_{-\infty}^{\infty} f(t)\, e^{-j\omega t}\, dt \tag{1.1}$$

where ω is a real parameter. Similarly the inverse Fourier transform of $F(\omega)$ is

$$\mathcal{F}^{-1}\{F(\omega)\} = f(t) = \frac{1}{2\pi} \int_{-\infty}^{\infty} F(\omega)\, e^{j\omega t}\, d\omega\,. \tag{1.2}$$

This transform may be written differently then that in (1.1)-(1.2): the coefficients 1.0 and $1/2\pi$ which multiply the integrals shown are not unique. However, the product of these two coefficients must be $1/2\pi$. The Fourier transform will not converge for a wide range of functions such as the positive exponential. Also, since the Fourier transform is a two sided transform, initial values are not readily recovered. However, [5] shows a method of modifying the Fourier transform so that it will converge for initial value problems, and as a result, they obtain the definition of the Laplace transform. Unfortunately, this modified Fourier transform or Laplace transform no longer has the simple inverse (1.2). References [1,2,3,9,10] contain rigorous theoretical development and general applications of the Fourier transform.

Laplace transform

Given f(t) a real or complex function of real variable t, the one sided Laplace transform of f(t) is, [5]

$$\mathscr{L}\{f(t)\} = F(s) = \int_0^\infty e^{-st} f(t)\, dt \tag{1.3}$$

where s is a complex parameter. Note that it is assumed that $f(t) = 0$ for $t < 0$ to ensure a one-to-one relationship between the Laplace domain and the time domain. Also, the region of convergence of f(t) is generally to the right of the line $Re(s) = k$ where k is finite.

The use of the Laplace transform in solving initial-value problems associated with ordinary linear differential equations is very common since differentiation in the time domain is converted into algebraic forms in the Laplace domain. Another desirable result of Laplace transformation is that convolution in the time domain is rendered as a product under the Laplace domain. Unfortunately the Laplace transform does not lend itself well to numerical operations. This point is further considered below. References [1,2,3,4,5] contain detailed information on the properties and the many applications of the Laplace transform.

Inverse Laplace transform

If F(s) is the Laplace transform of f(t) then the inverse transform is given by [5]

$$\mathscr{L}^{-1}\{F(s)\} = f(t) = \frac{1}{j2\pi} \int_{-j\infty + \sigma}^{j\infty + \sigma} F(s)\, e^{st} dt \tag{1.4}$$

where σ lies in the region of convergence. In contrast to the inverse Fourier transform the inverse Laplace transform is an integral in the complex plane. Evaluation by direct integration is almost always a complicated task. However, for functions of most interest in systems theory, the evaluation can be done by the determination of coefficients in the partial fraction expansion and using a Laplace transform table.

There are a number of Fortran subroutines that can be used to find the inverse Laplace transform of F(s). The routines in [6,7] use F(s) to approximate the Fourier series coefficients of f(t). The method in [6] has been implemented as an IMSL subroutine (IMSL is a commercially available library of Fortran subroutines). Unfortunately, the methods in [6,7] are not suitable for transforming F(s) to f(t) for large ranges of t. However, the method in [8] uses Laguerre polynomials to estimate f(t) and the authors claim that this

method is faster than the methods used in [6,7] and is well suited for transforming F(s) into f(t) over a large range of t.

Impulse response and convolution

Using equation (1.1), the Fourier transform of simple functions such as sin(t) and the step function u(t) does not exist in a strict mathematical sense. Therefore it is necessary to define the impulse function so that these and other functions can be included in the Fourier transform technique. The two defining properties of the impulse function $\delta(t)$ are [5]

$$\begin{aligned} &\delta(t) = 0 \quad \text{for} \quad t \neq 0 \\ &\int_{-\infty}^{\infty} \delta(t)\, dt = 1 \,. \end{aligned} \tag{1.5}$$

Then, by definition, the Fourier transform of $\delta(t)$ is

$$\mathcal{F}\{\delta(t)\} = \int_{-\infty}^{\infty} \delta(t)\, e^{-j\omega t}\, dt = 1 \tag{1.6}$$

and one deduces the value of the inversion integral as

$$\delta(t) = \mathcal{F}^{-1}\{1\} = \frac{1}{2\pi} \int_{-\infty}^{\infty} e^{j\omega t}\, d\omega \,. \tag{1.7}$$

Given a linear time invariant system with zero initial conditions, let y(t) be the response function resulting from a unit impulse function being applied as an input at $t = 0$. The function y(t) is called the impulse response of the system. If x(t) is an input function to the same system and v(t) is the resulting output function then [9]

$$v(t) = \int_{-\infty}^{\infty} x(\lambda)\, y(t - \lambda)\, d\lambda \,. \tag{1.8}$$

This integral is known as the convolution integral and is abbreviated as

$$v(t) = x(t) * y(t) \tag{1.9}$$

It can be shown that the Fourier transform of v(t) can be obtained from the product of the Fourier transform of the input function $X(\omega)$ and the Fourier transform of the impulse response $Y(\omega)$ [9],

$$V(\omega) \triangleq \mathcal{F}\{x(t) * y(t)\} = X(\omega)\, Y(\omega) \tag{1.10}$$

This property makes the Fourier transform very useful in circuit analysis. The same property, that is the rendering of convolution to a simple product, also occurs under Laplace transformation and certain other transforms.

Discrete Fourier transform (DFT)

The Fourier transform of a periodic function is a sequence of equidistant impulses. Likewise, the inverse Fourier transform of a periodic function is a sequence of equidistant impulses. Thus, with both the time function and its transform being periodic, all the information about both is limited to two finite sets of coefficients: the strengths of the impulse functions [1]. By definition, the discrete Fourier transform and inverse discrete Fourier transform are, [10]

$$F(k\Omega) = \sum_{n=0}^{N-1} f(n\Delta t)\, e^{-J\Omega\Delta tnk} \qquad k = 0,1,...,N-1 \tag{1.11}$$

$$f(n\Delta t) = \frac{1}{N} \sum_{k=0}^{N-1} F(k\Omega)\, e^{j\Omega\Delta tkn} \qquad n = 0,1,...,N-1 \tag{1.12}$$

where $F(k\Omega)$ is the DFT of $f(n\Delta T)$, and $f(n\Delta t)$ is the inverse DFT of $F(k\Omega)$. Also, $\Omega = 2\pi/N\Delta t$ is the separation of impulses in the frequency domain and Δt is the separation of impulses in the time domain. The ambiguity of the coefficient of the forward and reverse Fourier transform integrals also applies to (1.11) and (1.12). The DFT may be defined with other coefficients of the sum shown provided that their product is 1/N.

Convolution under the DFT

Similar to equation (1.10), convolution when using the DFT is

$$x(n\Delta t) * y(n\Delta t) = \sum_{i=0}^{N-1} x(i\Delta t)\, y[(n-i)\Delta t] \tag{1.13}$$

$$\mathcal{F}_D\{x(n\Delta t) * y(n\Delta t)\} = X(k\Omega)\, Y(k\Omega) \tag{1.14}$$

where $X(k\Omega)$ and $Y(k\Omega)$ are the DFT of $x(n\Delta t)$ and $y(n\Delta t)$ respectively [10].

Hartley transform

Given a real waveform $v(t)$ we define the Hartley transform pair

$$H(\omega) = \int_{-\infty}^{\infty} v(t)\, \mathrm{cas}\, \omega t\, dt$$

$$v(t) = \frac{1}{2\pi} \int_{-\infty}^{\infty} H(\omega)\, \mathrm{cas}\, \omega t\, dt$$

where cas refers to the cosine-and-sine function, $\mathrm{cas}\, \omega t \equiv \cos \omega t + \sin \omega t$. Note that the Hartley transform of $v(t)$ is $H(\omega)$ and that $H(\omega)$ is a real function [11,12]. The same ambiguity of coefficients noted earlier applies to the Hartley

transform.

The relationship between the Fourier transform and the Hartley is shown by first defining the even $E(\omega)$ and odd $O(\omega)$ parts of the Hartley transform of $v(t)$

$$E_v(\omega) = \frac{H_v(\omega) + H_v(-\omega)}{2} \tag{1.17}$$

$$O_v(\omega) = \frac{H_v(\omega) - H_v(-\omega)}{2} .$$

Then the Fourier transform of $v(t)$ is $V(\omega)$ where

$$V(\omega) = E_v(\omega) - j\ O_v(\omega) . \tag{1.18}$$

Also

$$H(\omega) = \text{real}\ (V(\omega)) - \text{imag}\ (V(\omega)) \tag{1.19}$$

where real$(\cdot)$ and imag$(\cdot)$ are the real and imaginary parts of the complex quantity.

Perhaps the most important difference between the Hartley transform and the Fourier transform is that the Hartley transform of $v(t)$ is always a real function, and the Fourier transform of $v(t)$ is in general, a complex function [8].

Convolution under the Hartley transform

Using (1.10) and (1.18), convolution in the Hartley domain is found as follows

$$V(\omega) = [E_x - jO_x]\ [E_y - jO_y]$$

from (1.19),

$$H_v(\omega) = [E_xE_y - O_xO_y] + [O_xE_y + E_xO_y]$$

thus, from (1.17)

$$H_v(\omega) = \frac{1}{2}\left[H_x(\omega)\,(H_y(\omega) + H_y(-\omega)) + H_x(-\omega)(H_y(\omega) - H_y(-\omega))\right] \tag{1.20}$$

where $H_v(\omega)$, $H_x(\omega)$, and $H_y(\omega)$ are the Hartley transforms of the output, input, and impulse response functions respectively, as defined in equation (1.8).

Discrete Hartley transform (DHT)

Analogous to the DFT, the discrete Hartley transform (DHT) and its inverse are given by [5],

$$H(k\Omega) = \sum_{n=0}^{N-1} v(n\Delta t)\ \mathrm{cas}\ (kn\Omega\Delta T) \qquad k = 0,1,...,N-1 \tag{1.21}$$

$$v(n\Delta t) = \frac{1}{N} \sum_{k=0}^{N-1} H(k\Omega)\ \mathrm{cas}\ (kn\Omega\Delta t)\,. \qquad n = 0,1,...N-1 \tag{1.22}$$

The even and odd parts of $H(k\Omega)$ are,

$$E(k\Omega) = \frac{H(k\Omega) + H[(N-k)\Omega]}{2} \tag{1.23}$$

$$O(k\Omega) = \frac{H(k\Omega) - H[(N-K)\Omega]}{2}\,.$$

One can find the DFT from the DHT by

$$F(k\Omega) = E(k\Omega) - j\ O(k\Omega)\,. \tag{1.24}$$

Conversely

$$H(k\Omega) = \mathrm{real}(F(k\Omega)) - \mathrm{imag}(F(k\Omega))\,. \tag{1.25}$$

Finally, convolution with the DHT is given by

$$H_v(k\Omega) = \frac{1}{2}\,[H_x(H_y + H_y(-)) + H_x(-)(H_y - H_y(-)]$$

where the subscripts are analogous to the subscripts is equation (1.20), $H_q(-) = H_q[(N-k)\Omega]$ with q = v, x,y, and $H_q = H_q(N\Omega)$.

Fast Fourier transform (FFT)

Perhaps the most significant advance in signal processing theory in the last 40 years is the formulation of the fast Fourier transform (FFT). The FFT is a time and memory efficient algorithm used to calculate the DFT. It is important to note that the success of the DFT in the solution of circuits problems is largely due to the FFT. The FFT is an exact evaluation of the DFT. The FFT algorithms employ symmetry of $e^{-j\frac{2\pi nk}{N}}$ in order to reduce the number of computations. The algorithms are grouped into two basic types: decimation in time and decimation in frequency. The difference between the two is the method in which the data sequences are divided into single point DFT's which require no multiplications. Most FFT algorithms require the number of data points N to be a power of 2 in order to simplify the

algorithm. This is called a radix-2 FFT algorithm. Radix-4, radix-8 and other radices are also used [13].

The relationship between the DFT and the DHT suggests that an analog may exist for the rapid calculation of the DHT. This is indeed the case. Reference [14] shows that the philosophy used in the FFT can be used in computing the DHT.

1.3 Literature Summary of Some Methods for Calculating the Propagation of Non-Sinusoidal Waveforms in Power Systems

The solution to the well known second order linear differential equations obtained for a transmission line can be decomposed into two components which can be interpreted as reflected and incident traveling waves. There are numerous digital programs that use traveling wave methods to solve electromagnetic transient problems on power systems. The most widely used is the electromagnetic transient program EMTP developed by Bonneville Power administration. The method entails writing a system of linear algebraic equations for networks containing inductances, resistances, capacitances, and transmission lines. This is accomplished by replacing each element of the network with its equivalent conductance model and then writing the nodal equations for the new network. The nodal voltages are then calculated using the trapezoidal rule of integration in the time domain. Transmission lines are handled using Bergeron's characteristic impedance method. The time delays imposed by the traveling waves on the transmission lines using Bergeron's method require that information from previous integration steps be stored and used in later integration steps. References [15,16] contain detailed descriptions of the techniques used in EMTP. The main advantages of EMTP are:

- It can handle large scale systems
- It can include: nonlinearities, switches, and initial conditions
- It can include a wide variety of current and voltage excitation waveforms.

Unfortunately, EMTP is a numerically cumbersome program. The program employs a simple numerical integration routine so small time steps must be taken. In addition a constant time step must be used since the traveling waves require the program to use previous integration data. If three phase circuits are analyzed, the method uses constant transformation matrices to decouple the phases. Problems arise in dealing with frequency dependent parameters and constant transformation matrices [17].

Transform methods for faulted transmission lines

The problems encountered with frequency dependent parameters in the traveling wave methods can be solved by working in the frequency domain. Sources in the literature [17-19] show how both the distributed and frequency dependent parameters of a single transmission line can be considered when working in the frequency domain. In general the methods entail working in the Laplace domain and then computing the inverse Laplace transform by truncating the frequency range of the system and using the FFT. The frequency range of the Laplace function is truncated by multiplying it by

$$\sigma(\omega) = \frac{\sin(\omega\pi/\Omega)}{\omega\pi/\Omega} \tag{1.27}$$

where ω is the frequency variable and Ω is the cutoff frequency. Then frequency samples of the truncated function are taken and an FFT algorithm is used to find the corresponding time samples. However, [17-19] concentrate on faulted systems and switching operations only.

For short line distribution systems and low frequencies (i.e. below 10 kHz) lumped parameter models of the power system are sufficient [20]. Therefore, basic circuit analysis techniques can be used to analyze these models.

State equations and numerical integration

The state equations for a lumped parameter model of a distribution system can be written as

$$\frac{dx}{dt} = A\,x(t) + Br(t) \tag{1.28}$$

where r(t) is the input vector, x(t) is the state vector, and A and B are constant matrices. A time step solution such as Euler's method or the Runge-Kutta method can be used to solve for x(t). Unfortunately, for a system with n energy storage elements dx/dt will be an n-vector and n differential equations must be solved even if all that is needed is one node voltage [21]. Other problems with time step solutions to differential equations are numerical roundoff error and numerical instability. In addition, in order to recover all of the high frequency detail of the actual solution the time-step must be very small making computation times very long.

Improved time solution methods

By employing some approximations and efficient algorithms time-step solutions can be made more feasible. One method of reducing the number of points to be computed is to predict the time step for the next point by looking at the changes between the previous points. This way during relatively smooth regions of the function, the computer can move along quickly and when rapid changes occur in the function, the computer can reduce the time step so it can still closely estimate the function. Relative accuracies can be obtained by checking such parameters as loop equations at each point calculated, and if the specified accuracy is not met at a specific point the step can be reduced and that point can be recalculated. Another improvement is to linearize the circuit at each point. For example, at each iteration each capacitor and inductor can be modeled as a voltage and current source respectively, with a resistance. By doing this modeling the network can be represented as a set of linear equations to be solved at each point. The most well known program that uses techniques like those discussed above is the SPICE program [22].

1.4 Organization of This Thesis

Time domain solution methods for determining transients in power systems are well known. The research done in this thesis concentrates on *frequency domain* methods. Chapter II discusses the theory used to formulate solution methods using the Laplace transform, the Fourier transform, and the Hartley transform. The Laplace transform method relies on using a numerical inverse Laplace transform routine. The performance of the routine for this application is evaluated. The Fourier and Hartley transform techniques rely on the existence of fast discrete Fourier, and Hartley transforms respectively. Chapter III contains the solution of an eight bus system which is representative of a power system. The node voltages due to a nonsinusoidal current injection are calculated. The problem is solved using the Laplace transform, the Fourier transform, and the Hartley transform. The results are verified by solving the problem using the commercial time domain simulation routine SPICE.

Chapter IV starts with a discussion on the modeling of a power system for the analysis of the propagation of nonsinusoidal waveforms. This chapter also demonstrates the sensitivity of the circuit solution to the model parameters and the injection current characteristics.

In Chapter V the advantages and disadvantages of the different methods are discussed. Also, some recommendations are made on further required research.

CHAPTER II
PROBLEM FORMULATION AND SOLUTION

2.1 Calculation of Transfer Impedances

The problem to be solved is the following: given a power system with nonsinsoidal current injections, find the bus voltages resulting from this injected current. It is assumed that the power system is approximately linear. Under this assumption the 60 Hz component is omitted and can be superimposed on the final solution. More importantly the linearity allows this problem to be solved by convolving the injected current i(t) with an impulse response of the power system z(t) using (1.8). The impulse response required is the voltage response at the node of interest due to a current impulse applied at the bus where the injected current is applied. However, convolution is simplified by transforming to the frequency domain and using (1.10). The three methods of transforming to the frequency domain that are discussed here are the Laplace transform, the Fourier transform, and the Hartley transform.

When an impulse response z(t) is transformed to the frequency domain it is called a transfer function. The transfer function needed for this problem is the transfer function between the current applied at one bus and the voltage response at another bus. This is called the transfer impedance $Z(\omega)$.

Given an n bus system the bus impedance matrix used in power systems, Z_{bus}, is defined in [23] as

$$(Z_{bus})_{ij} = \frac{\partial V_i}{\partial I_j} \qquad i = 1,2,...,n \qquad j = 1,2,...,n\,. \tag{2.1}$$

An important property of Z_{bus} is that its off diagonal entries are the transfer impedances and its diagonal entries are the driving point impedances of the system. Therefore the bus voltages due to the injection currents can be calculated by

$$V_{bus} = Z_{bus}\, I_{bus} \tag{2.2}$$

where V_{bus} is a vector containing the n bus voltages, I_{bus} is a vector containing the n current injections, and Z_{bus} is the n×n impedance matrix. The impedance matrix Z_{bus} can be found by inverting the admittance matrix Y_{bus}.

Alternatively, Z_{bus} can be found by using the Z_{bus} building algorithm discussed in [23]. An approximation of Z_{bus} that can be rapidly calculated will be discussed later.

2.2 Laplace Transform Method

An n bus power system can be converted to an n bus s-domain equivalent circuit. The equivalent circuit for each circuit element is developed by finding the relationship between the elements s-domain terminal voltage and current [24]. The rules for combining impedances and admittances in the s domain are the same as those for combining impedances and admittances in phasor domain circuits. Another important observation is that Kirchoffs laws still hold for the s-domain equivalent circuit. This is because the sum of the time domain functions is the sum of the transforms of the individual functions [24]. Therefore (2.2) can be written as

$$V_{bus}(s) = Z_{bus}(s)I_{bus}(s) \tag{2.3}$$

where

$$(Z_{bus}(s))_{ij} = \frac{\partial V_i(s)}{\partial I_j(s)} \qquad i = 1,2,...,n \qquad j = 1,2,...,n \tag{2.4}$$

and $V_{bus}(s)$, $I_{bus}(s)$ are vectors containing the s-domain node voltages and current injections.

The injected current although nonsinusoidal will be periodic. The Laplace transform of the periodic time function can be found from

$$I(s) = \frac{I_1(s)}{1 - e^{-Ts}} \tag{2.5}$$

where $I_1(s)$ is the Laplace transform of one period of i(t) and T is the length of one period in seconds. $I_{bus}(s)$ is found by using (2.5) on the injection current at each bus. With $I_{bus}(s)$ and $Z_{bus}(s)$, $V_{bus}(s)$ is determined from (2.3). Then v(t) at each bus is calculated by taking the inverse Laplace transform of each element in $V_{bus}(s)$. Unfortunately, for reasonably complicated injection currents and multiple bus systems, finding V(s) by hand calculation is not feasible. Furthermore, finding v(t) by partial fraction expansion is also not feasible for reasonably complicated systems. Alternatively, a solution by digital computer is used. This is done by evaluating $Z_{bus}(s)$ and $I_{bus}(s)$ at different values of s. Then multiplying them to find $V_{bus}(s)$ at these values of s. The Fourier series coefficients of v(t) can then be approximated by the routines discussed in section 1.2.

2.3 Fourier Transform Method

Given an s-domain function F(s) the corresponding Fourier transform function $F(\omega)$ will exist if all the poles of F(s) lie in the left half of the s-plane. If f(t) the corresponding time function is zero for $t \leq 0^-$, the Fourier transform of f(t) can be found by simply replacing s in F(s) by $j\omega$. Therefore if f(t) is zero for negative-time and has no initial conditions, $F(\omega)$ can be easily found from F(s). Since our n-bus power system is a causal system with zero initial conditions the impulse responses of the system are zero for $t \leq 0^-$. Hence $Z_{bus}(\omega)$ can be found by substituting $j\omega$ for s in $Z_{bus}(s)$ [24]. Note that when F(s) contains $j\omega$ axis poles, $F(\omega)$ may also exist. Under such circumstances, $F(\omega)$ contains singularity functions of $\omega - \omega_p$ where ω_p is the pole location of F(s). In practical power systems, F(s) rarely contains axis poles, and this case will not be considered further.

In order to use the convenience and speed of the digital computer, attention is now turned to the discrete Fourier transform. Let $i(n\Delta t)$ contain N samples taken every Δt seconds of an injection current i(t). Let $I(k\Omega)$ contain the frequency samples obtained by taking the DFT of $i(n\Delta t)$. Note that $\Omega = 2\pi/N\Delta t$ is the separation of the frequency samples and $\Omega_{max} = (N/2)\Omega$ is the highest frequency recovered from the function i(t). The reason for the $(N/2)\Omega$ instead of $N\Omega$ is that the periodicity of the discrete Fourier function places the negative frequency samples in the N/2 to N-1 positions of $I(k\Omega)$. In order to insure an accurate solution for the node voltages the rate of sampling, Δt, must be small enough so that Ω_{max} includes the significant part of the frequency spectrum of the injection current. Thus, the discrete Fourier transform of i(t) is found by first sampling i(t) and then transforming those samples to the frequency domain using the DFT. This process is performed on the injection currents of every bus to obtain $I_{bus}(k\Omega)$.

The process for finding the discrete Fourier transform of the transfer impedances is different from the process of finding the DFT of the injection currents. This is because the continuous Fourier transform of the transfer impedance is already known. Therefore the discrete Fourier transform of the transfer impedance $Z(k\Omega)$ is found by sampling $Z(\omega)$ in the frequency domain. In order for $Z(k\Omega)$ to be a discrete Fourier transform it must be a representative period of the periodic function obtained by replicating the samples of $Z(\omega)$ every $N\Omega$ rad/sec. This is done by placing the positive frequency samples in the 0 to $N/2 - 1$ positions and the negative frequency samples in the N/2 to N—1 positions in reverse order. The N/2 entry is an indeterminate value and can be set to zero for convenience. For an N point discrete Fourier transform, $Z(\omega)$ needs to be sampled only N/2 times. The

other N/2 samples or the negative frequency samples are simply the conjugate of the positive frequency samples. This fact produces a significant computational savings.

The frequency resolution Ω of the samples of $Z(\omega)$ is controlled by the number of samples N. The spectrum for each periodic, injected current will have nonzero samples only at their respective harmonic frequencies. Therefore samples of $Z(\omega)$ need to be taken only at these harmonic frequencies.

Another important consideration when choosing N and Δt is the length of time that i(t) the injection current is sampled. The order of magnitude of Δt is dictated by aliasing considerations of $I(k\Omega)$. In order to use radix 2 methodologies, the value of N must be a power of 2. The product $t_f = N\Delta t$ is the length of time that i(t) is sampled. Moreover, the injection current i(t) is a periodic function, and a steady state value of the node voltages is the information that is required. Therefore t_f must be equal to an integer multiple of the period T of the injection current function i(t). If t_f is not an integer multiple of T, then the samples in the frequency domain, of the injection current will be from a time function of period t_f, and this function is completely different than the periodic function i(t) of period T actually injected.

Finally, one must consider practical limits on the value of N so that computation is not excessive.

The process for finding the discrete Fourier transform of a transfer impedance is applied to every element in $Z_{bus}(\omega)$ to obtain $Z_{bus}(k\Omega)$. For $Z_{bus}(k\Omega)$ and $I_{bus}(k\Omega)$ to be convolved to find $V_{bus}(k\Omega)$ it is essential that the number of frequency samples N and the spacing of the samples be the same for every element in $Z_{bus}(k\Omega)$ and $I_{bus}(k\Omega)$. With this requirement satisfied $V_{bus}(k\Omega)$ can be found from

$$V_{bus}(k\Omega) = Z_{bus}(k\Omega)I_{bus}(k\Omega) \qquad k = 0,1,...,N-1 \; . \tag{2.6}$$

Then the time samples of each node voltage can be found by taking the inverse DFT of each element in $V_{bus}(k\Omega)$. A block diagram of the complete process is shown in Figure 2.1.

Errors introduced by the Fourier method

The process of time domain sampling i(t) results in frequency domain aliasing. This is evidenced by the overlapping versions of $I(\omega)$ which make up the discrete time Fourier transform $I_D(e^{j\omega})$ of the sampled signal (see Figure 2.2). Note that T_s in Figure 2.2 is the same as Δt. As stated before, this aliasing is reduced to a negligible problem by making T_s small thereby making

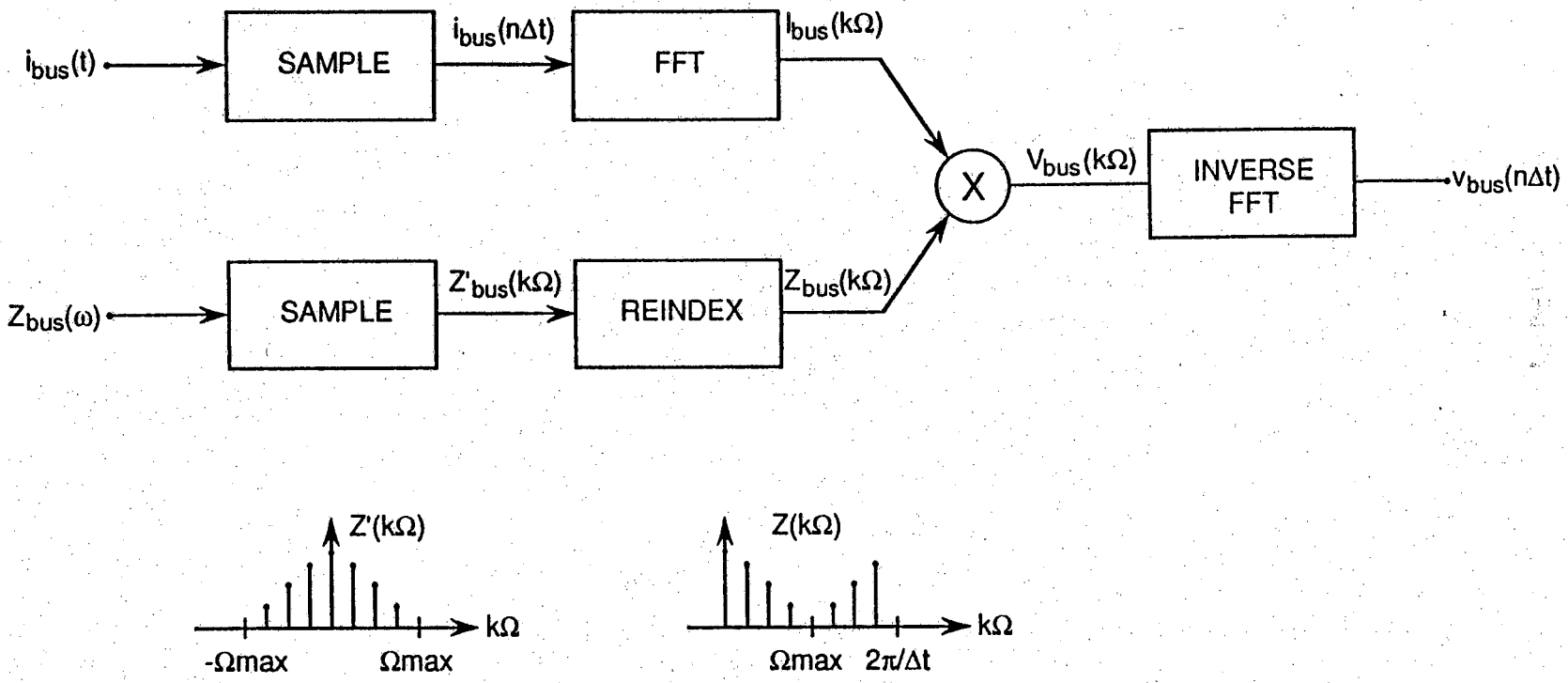

Figure 2.1 Block diagram of the Fourier transform method.

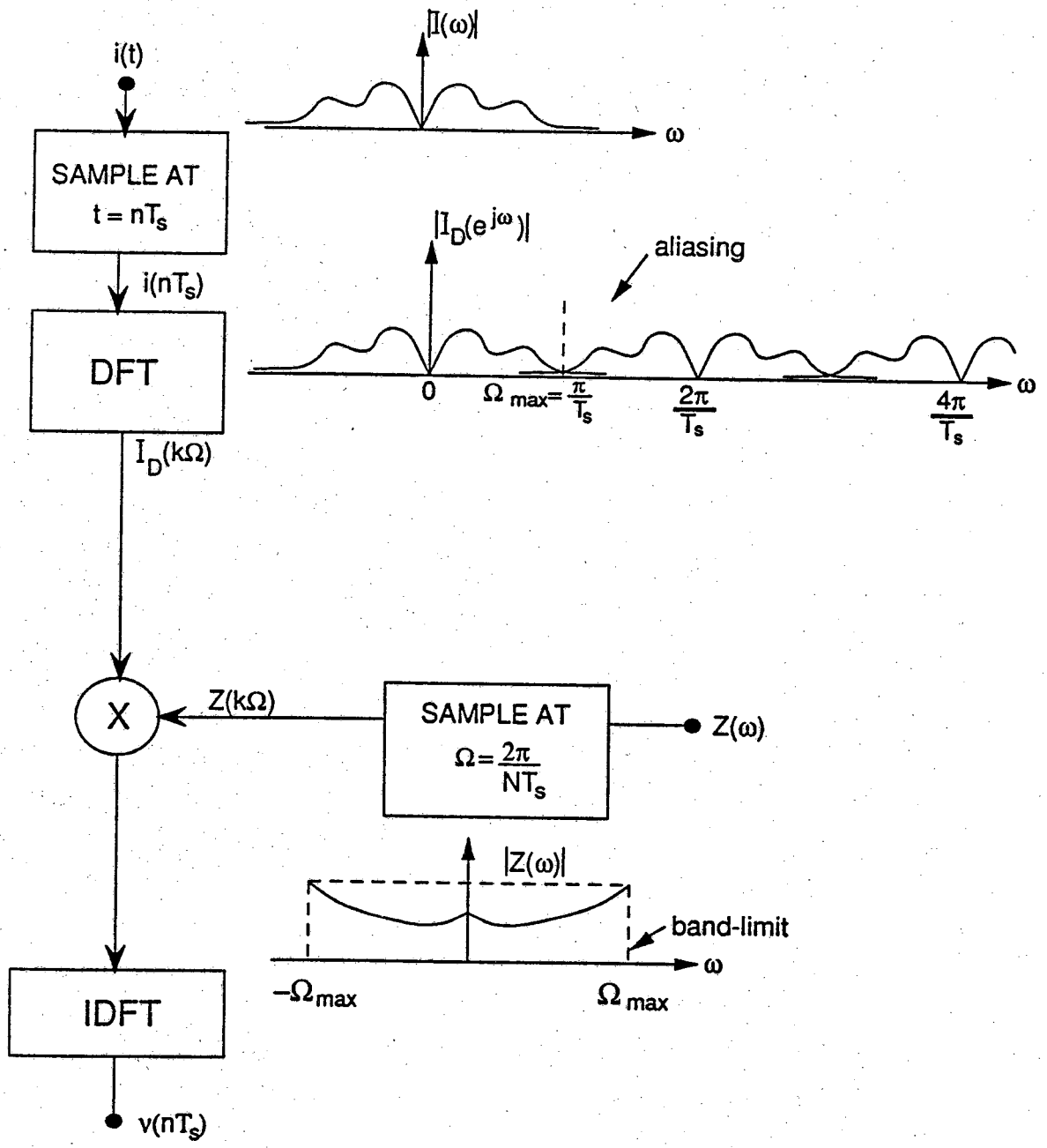

Figure 2.2 Illustration of the errors introduced by the Fourier transform method.

Ω_{max} large enough so that the overlapping region is relatively small.

Time domain aliasing is introduced when sampling $Z(\omega)$. If the impulse response time duration is long this time domain aliasing could be a problem. However, this problem can be reduced by increasing the number of samples N.

Frequency domain aliasing is not a problem when obtaining the samples of $Z(\omega)$, and the function can be bandlimited to Ω_{max} which is the value obtained when sampling i(t). This bandlimiting introduces what is known as time domain smoothing. This problem will be negligible because the convolution process of $I(k\Omega)$ and $Z(k\Omega)$ bandlimits Z anyway [25].

2.4 Hartley Transform Method

By sampling the injection currents at the buses the same way they were sampled in the Fourier transform case and taking the discrete Hartley transform of these discrete functions, $[H_i(k\Omega)]_{bus}$ is obtained. The purely real vector $[H_i(k\Omega)]_{bus}$ is the discrete Hartley transform representation of the injection currents. It is clear from the relationships between the Hartley transform and the Fourier transform that the requirements for minimizing aliasing and other errors are identical for both transforms. Thus the choice of Δt the sample spacing is the same in the Hartley transform method as in the Fourier transform method.

Given $Z_{bus}(k\Omega)$ obtained by the method described earlier, $[H_Z(k\Omega)]_{bus}$ can be obtained by applying (1.25) to every element in $Z_{bus}(k\Omega)$. The purely real matrix $[H_Z(k\Omega)]_{bus}$ is Z_{bus} in the discrete Hartley transform domain. The discrete Hartley transform of the node voltages $[H_v(k\Omega)]_{bus}$ is now obtained by

$$H_v^{bus} = \frac{1}{2}\,[H_z^{bus}(H_i^{bus} + H_i^{bus}(-)) + H_z^{bus}(-)(H_i^{bus} - H_i^{bus}(-))] \qquad (2.7)$$

where $H_q^{bus} = [H_q(k\Omega)]_{bus}$, and $H_q^{bus}(-) = [H_q[(N-k)\Omega]]_{bus}$, $k = 1,2,...,N-1$, $q = v,z,i$. Then the voltage at each bus can be found by taking the inverse DHT of each component in H_v^{bus}.

CHAPTER III
DEMONSTRATION OF THE FREQUENCY DOMAIN METHODS

3.1 The Example System

In this chapter an example system which is representative of a power system is studied. The example will be studied using a numerical Laplace transform method, the FFT, and the fast Hartley transform. Also a time integration solution will be used to check and compare solution characteristics. Figure 3.1 shows the eight bus example system. General remarks on system component models appear in Chapter IV. However, the following remarks will help to introduce this example:

- Line charging is modelled as a lumped parameter at each system bus.
- Fixed R, L are used for transmission line models (i.e., the pi model is used).
- The connection from bus 1 to the remainder of the network is modelled as the equivalent negative sequence impedance $0.1 + j0.1$. This is conveniently found from the short circuit study of the external network.
- Loads are modelled as fixed resistances in this example.
- Mutual coupling is included.
- The distribution transformer at bus 6 is modelled as a fixed R-L T-equivalent. Frequency dependence is not included in this example.
- Turn-to-turn and interwinding capacitance of the transformer are modeled by fixed lumped capacitors.
- The 60 Hz sinusoidal supply at bus 1 is not included.

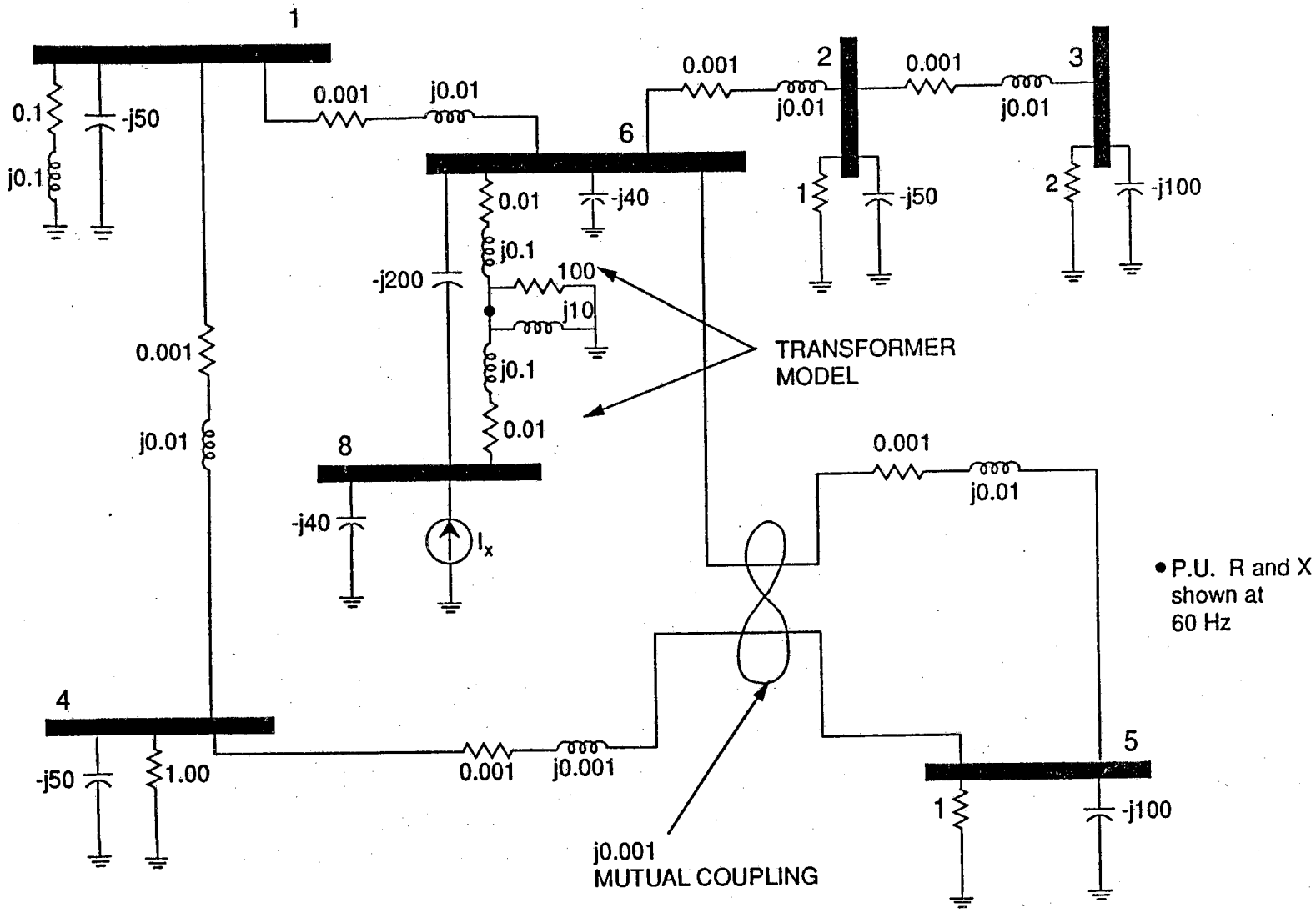

Figure 3.1 The example power system.

3.2 Laplace Transform Solution

In this section the bus voltages on the system in Figure 3.1 are calculated using the Laplace transform. Figure 3.2 depicts the nonsinusoidal current that is injected into bus 8. The matrix $Z_{bus}(s)$ is formed by building and inverting $Y_{bus}(s)$. The matrix $Y_{bus}(s)$ is easily constructed from the s-domain equivalent circuit of Figure 3.1. A method for incorporating the mutual inductance is covered in [26]. Using (2.5), the elements of $I_{bus}(s)$ are,

$$I_k(s) = 0 \qquad k = 1,2,...7$$

$$I_8 = [240(1 - e^{-t3s}) + 2000(e^{-t2s} - e^{-t5s}) - 2240(e^{-t4s} - e^{-t1s})]/s^2(1 - e^{-t6s}) \; . \tag{3.1}$$

The system node voltages which are contained in $V_{bus}(s)$ are found from

$$V_{bus}(s) = Z_{bus}(s)\, I_{bus}(s). \tag{3.2}$$

Using the numerical inverse Laplace transform routine discussed in [3] v(t) at each bus is computed from $V_{bus}(s)$. Figure 3.3 shows the voltage $v_1(t)$ at bus 1. Note that the s-domain equivalent circuit contained zero initial conditions so Figure 3.3 is the zero state solution. The piecewise-linear property of the injection current allows the problem to be solved by SPICE. Figure 3.4 shows the SPICE solution. The largest discrepancy between the two solutions for the interval shown is about 2%.

3.3 Fourier Transform Solution

In this section the example system is analyzed using the Fourier transform. The Fourier transform of Y_{bus} is found by setting $s = j\omega$ in $Y_{bus}(s)$. The discrete Fourier transform of Y_{bus} is found by substituting in values of ω every Ω rad/sec. Then $Z_{bus}(k\Omega)$ is found by inverting $Y_{bus}(k\Omega)$. The current $I_8(k\Omega)$ is found by sampling the injection current and taking the DFT of the samples. The other elements of $I_{bus}(k\Omega)$ are zero. The DFT of the bus voltages are found from

$$V_{bus}(k\Omega) = Z_{bus}(k\Omega) I_{bus}(k\Omega). \tag{3.3}$$

The bus voltages are then found by taking the inverse DFT of the elements of $V_{bus}(k\Omega)$. Exactly two periods of the injection current are sampled so a steady state solution for the voltages is obtained. Figure 3.5 shows the voltage at bus 1. The steady state SPICE solution is shown in Figure 3.6.

The zero state solution obtained by the Laplace transform method can also be obtained by the Fourier transform method. This is done by zero

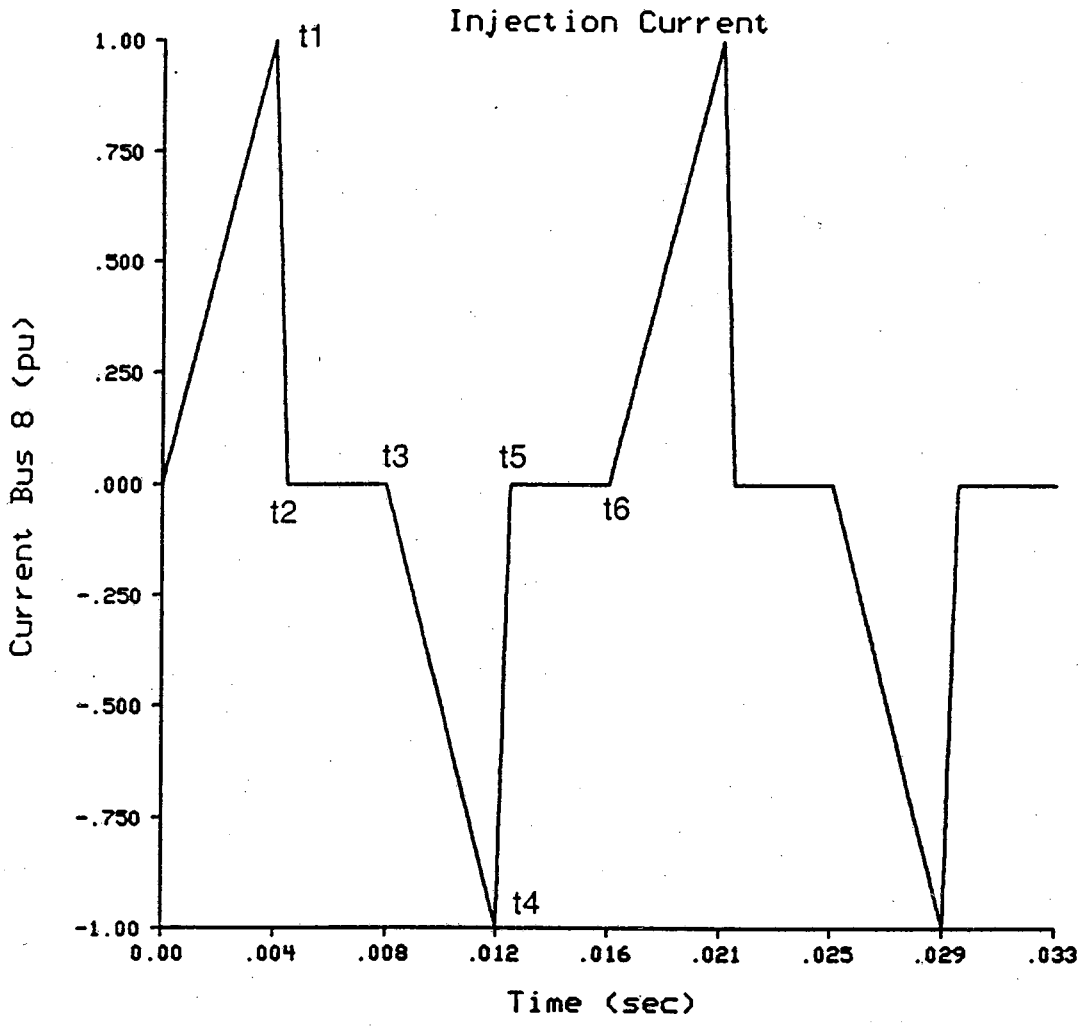

Figure 3.2 The nonsinusoidal current injected into bus 8.

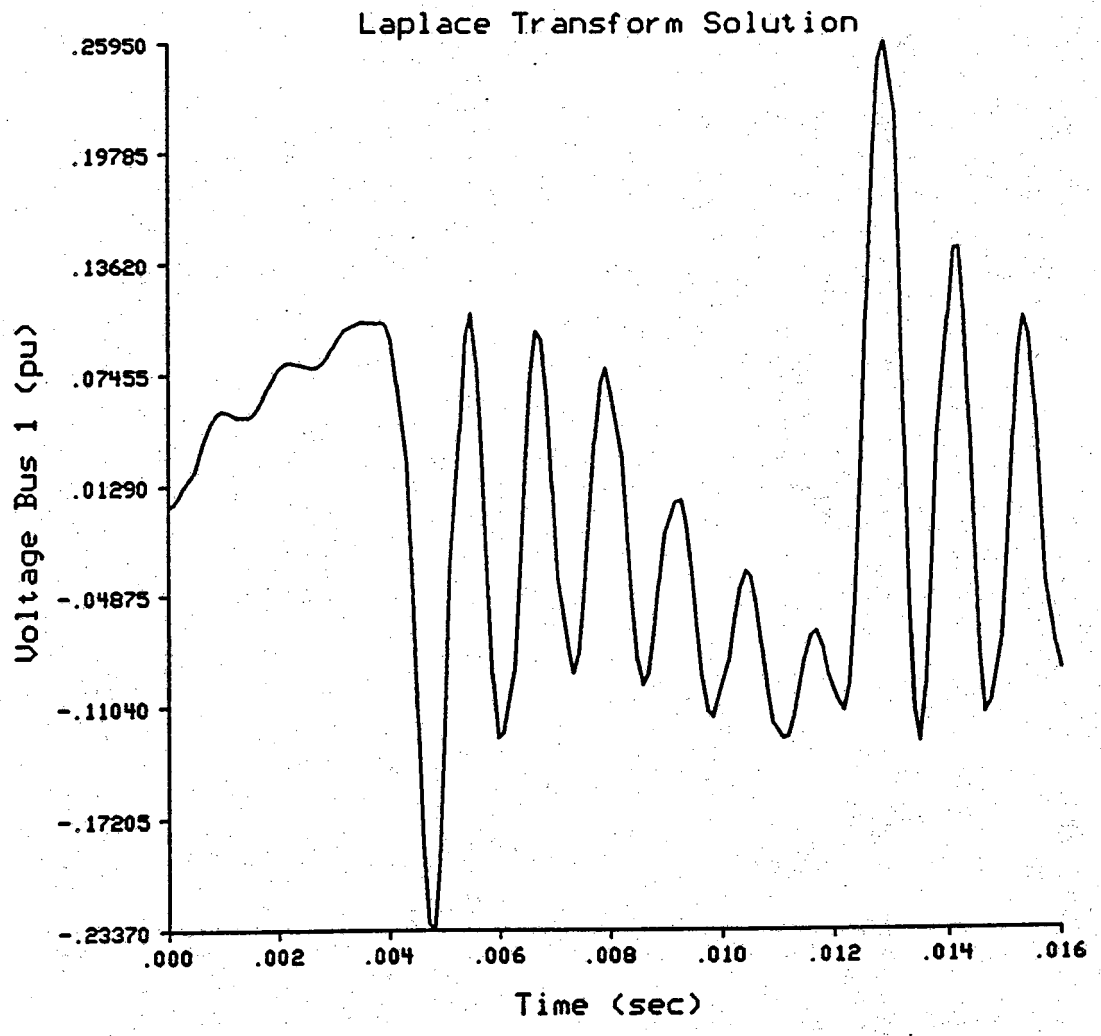

Figure 3.3 Laplace transform solution of the voltage at bus 1.

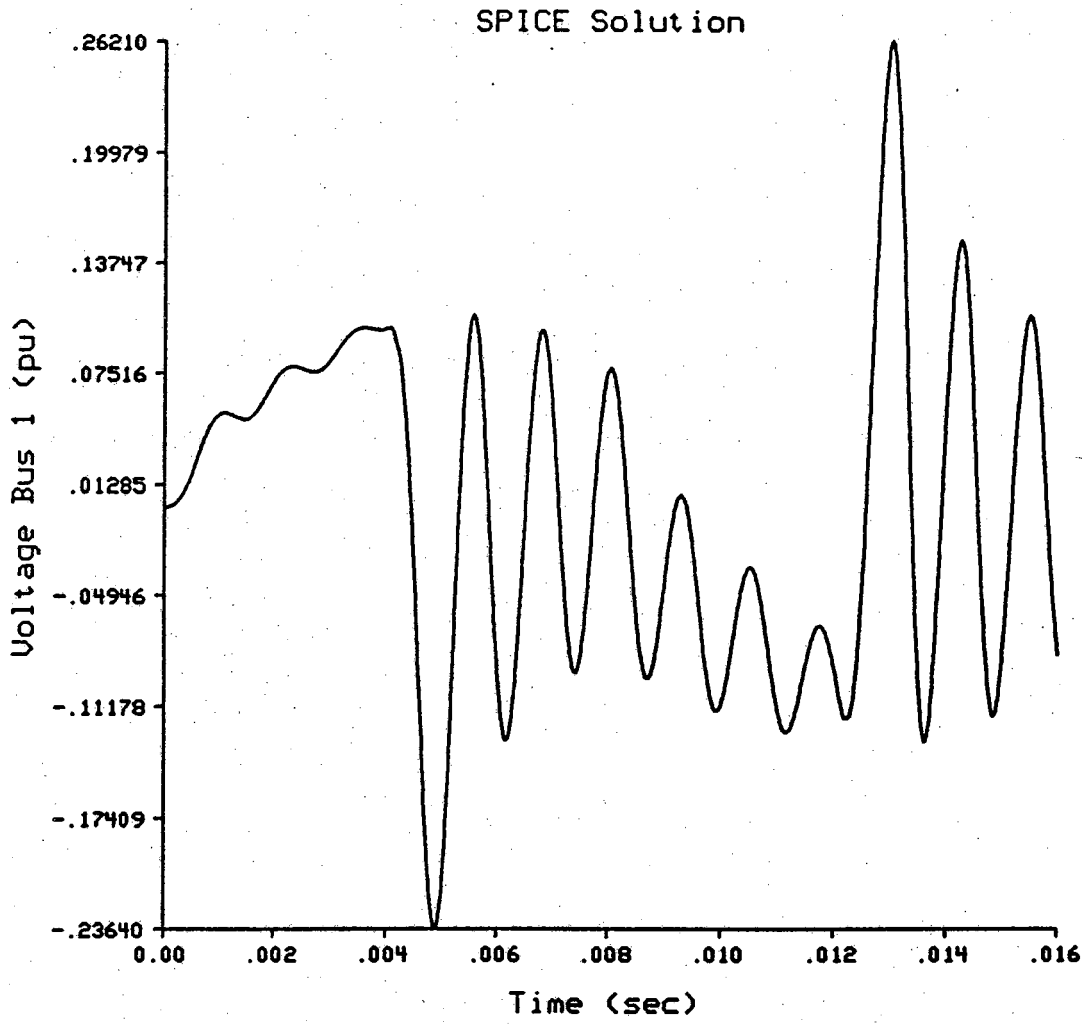

Figure 3.4 SPICE solution of the voltage at bus 1.

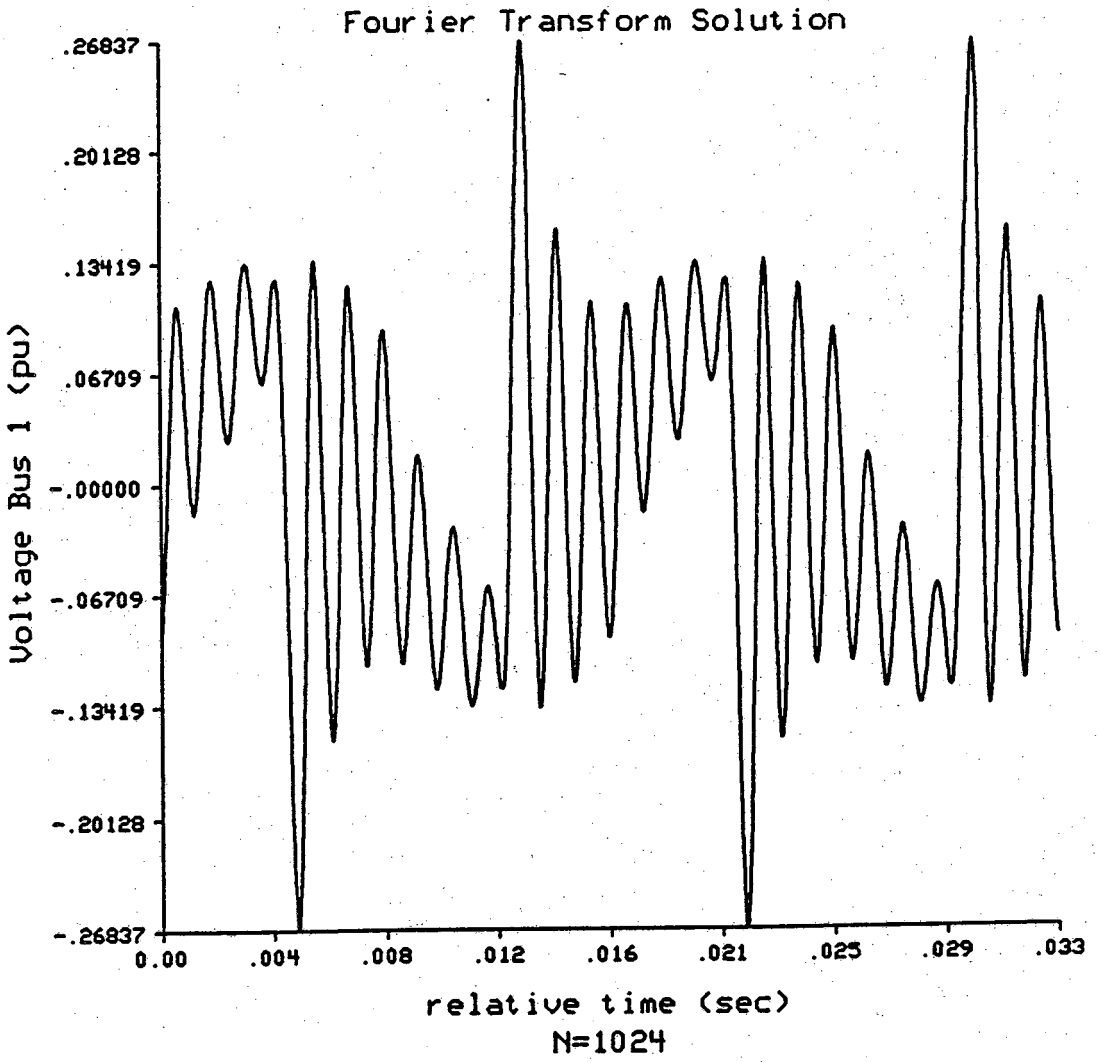

Figure 3.5 Fourier transform solution of steady state voltage at bus 1.

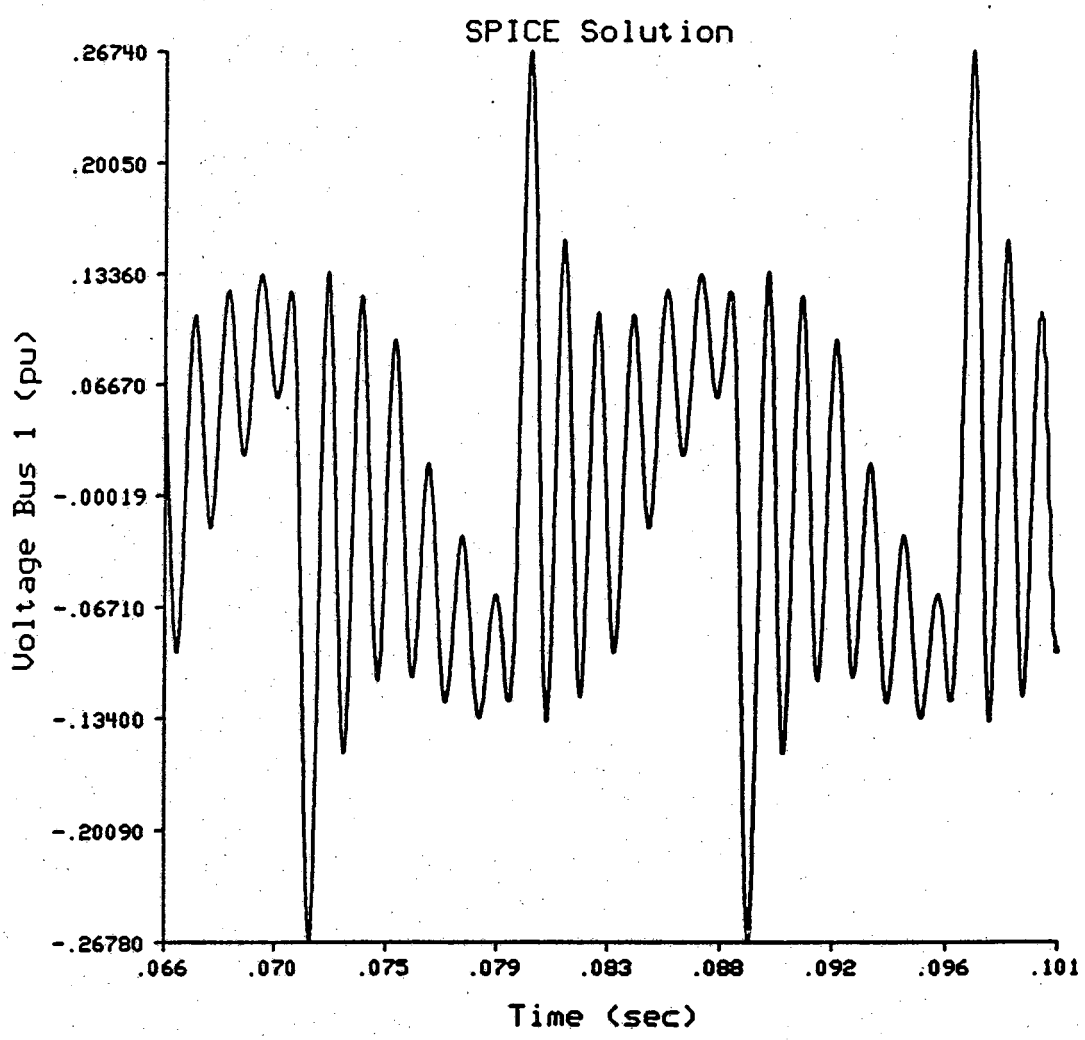

Figure 3.6 SPICE solution of steady state voltage at bus 1.

packing the latter part of $i_8(n\Delta t)$ long enough for $v_1(n\Delta t)$ to settle to zero by the end of the sample range. Figure 3.7 shows how $v_2(n\Delta t)$ settled out by zero packing $i_8(n\Delta t)$ after 0.0167 seconds. Figure 3.8 shows the first 0.0167 seconds of Figure 3.7. Comparing Figure 3.8 to the Laplace solution in Figure 3.3 shows that they are the same. The largest discrepancy between the two is about 2%.

Any injection current waveform can be analyzed using the Fourier transform method. Figure 3.9 shows an injection current that is similar to the piecewise-linear current, but Figure 3.9 has a rise proportional to t^3. The voltage at buses 1 and 8 due to the current in Figure 3.9 are shown in Figures 3.10 and 3.11 respectively. The low impedance ties between buses 1-6 keep the voltages at these buses practically the same. Therefore the voltage waveforms on buses 2-6 are not shown.

3.4 Hartley Transform Solution

After the manipulation of $Z_{bus}(k\Omega)$ to obtain $[H_z(k\Omega)]_{bus}$, the discrete Hartley transform of Z, the calculation of the bus voltages using the fast Hartley transform is accomplished using only real operations. The fast Fourier transform requires complex operations. Thus the Hartley transform is computationally more efficient than the Fourier transform. The procedure for the Hartley transform solution is analogous to the procedure for the Fourier transform solution, and the solution obtained was exactly the same for both methods. Figure 3.12 shows the Hartley transform representation of the transfer impedance between buses one and eight. Figures 3.13 and 3.14 show the magnitude and phase of the Fourier transform representation of the same transfer impedance. Note that it requires two graphs to represent the Fourier transform information and only one graph to depict Hartley transform information.

3.5 Choice of Sampling Parameters

The choice of the number of samples and the resolution of the samples is very important in discrete transform analysis. The following parameters must be specified before the discrete transform methods can be implemented:

t_f — length of time the injection current is sampled

Ω_{max} — maximum frequency sampled on the transfer impedances

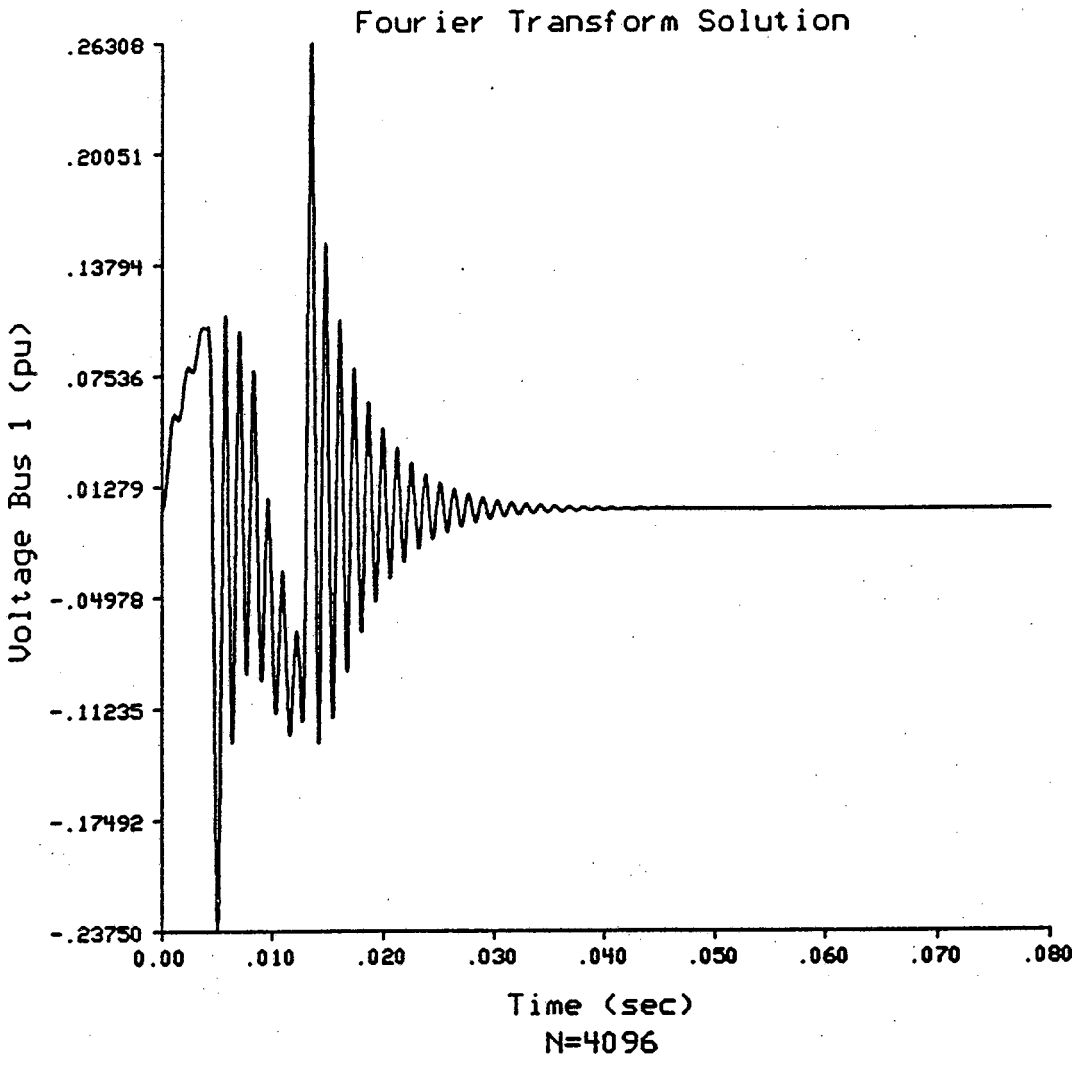

Figure 3.7 Fourier transform zero initial state solution at bus 1. Found by zero packing the current waveform samples after 0.0167 seconds.

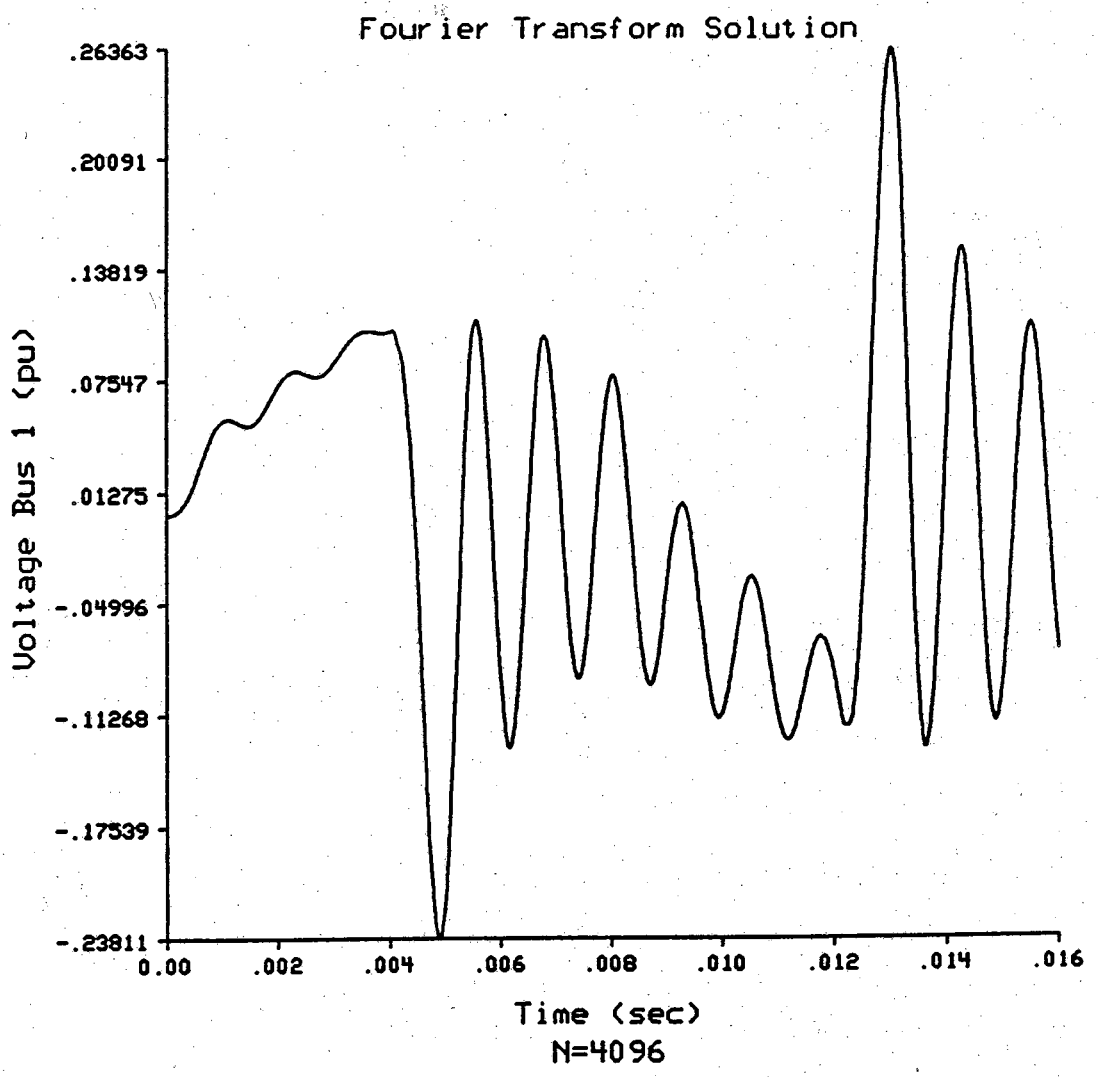

Figure 3.8 Fourier transform zero initial state solution at bus 1. The first 0.0167 seconds of Figure 3.7.

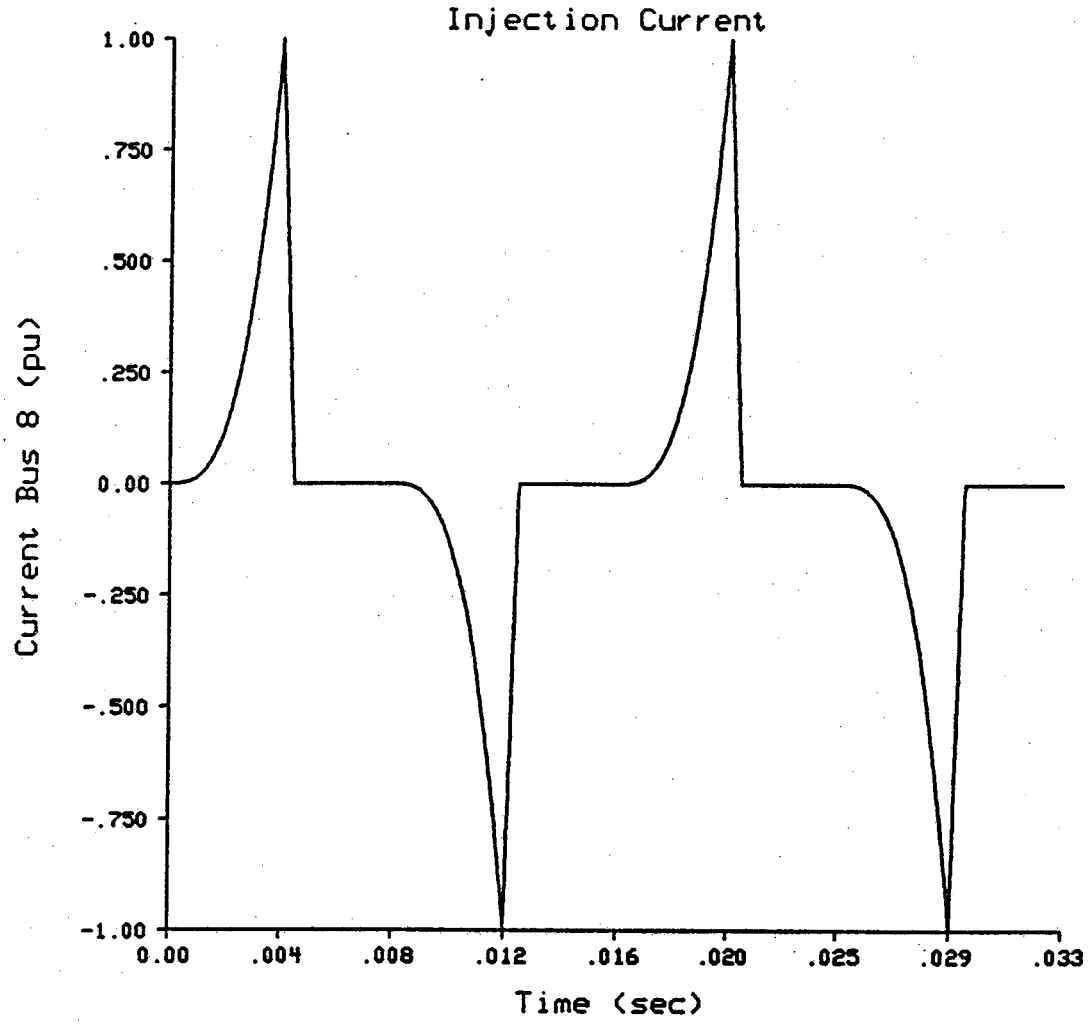

Figure 3.9 Injection current with a rise proportional to t^3. This current will be used in studies from this point on. This current is injected into bus 8.

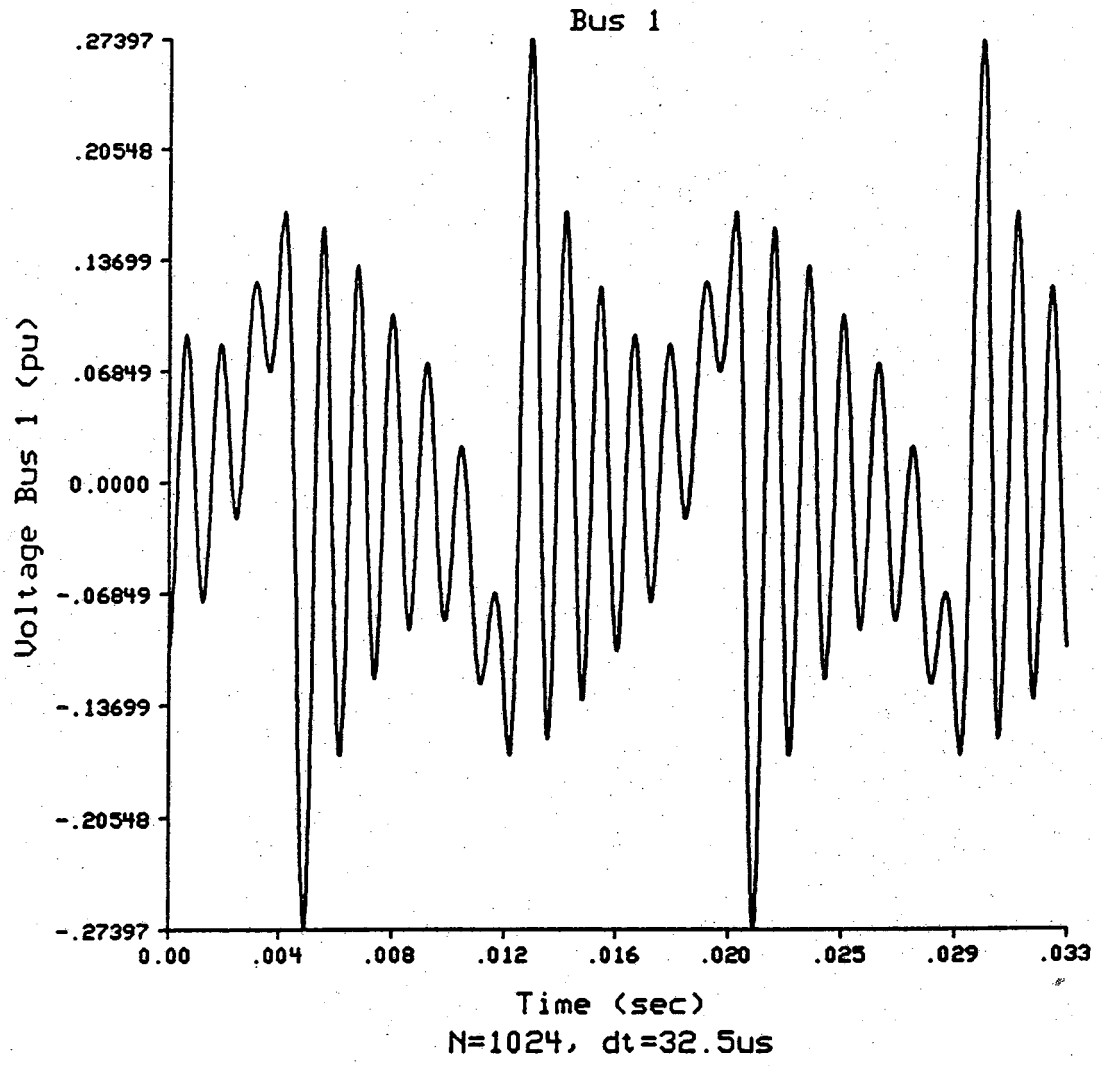

Figure 3.10 Fourier transform solution of steady state voltage at bus 1 due to current in Figure 3.9.

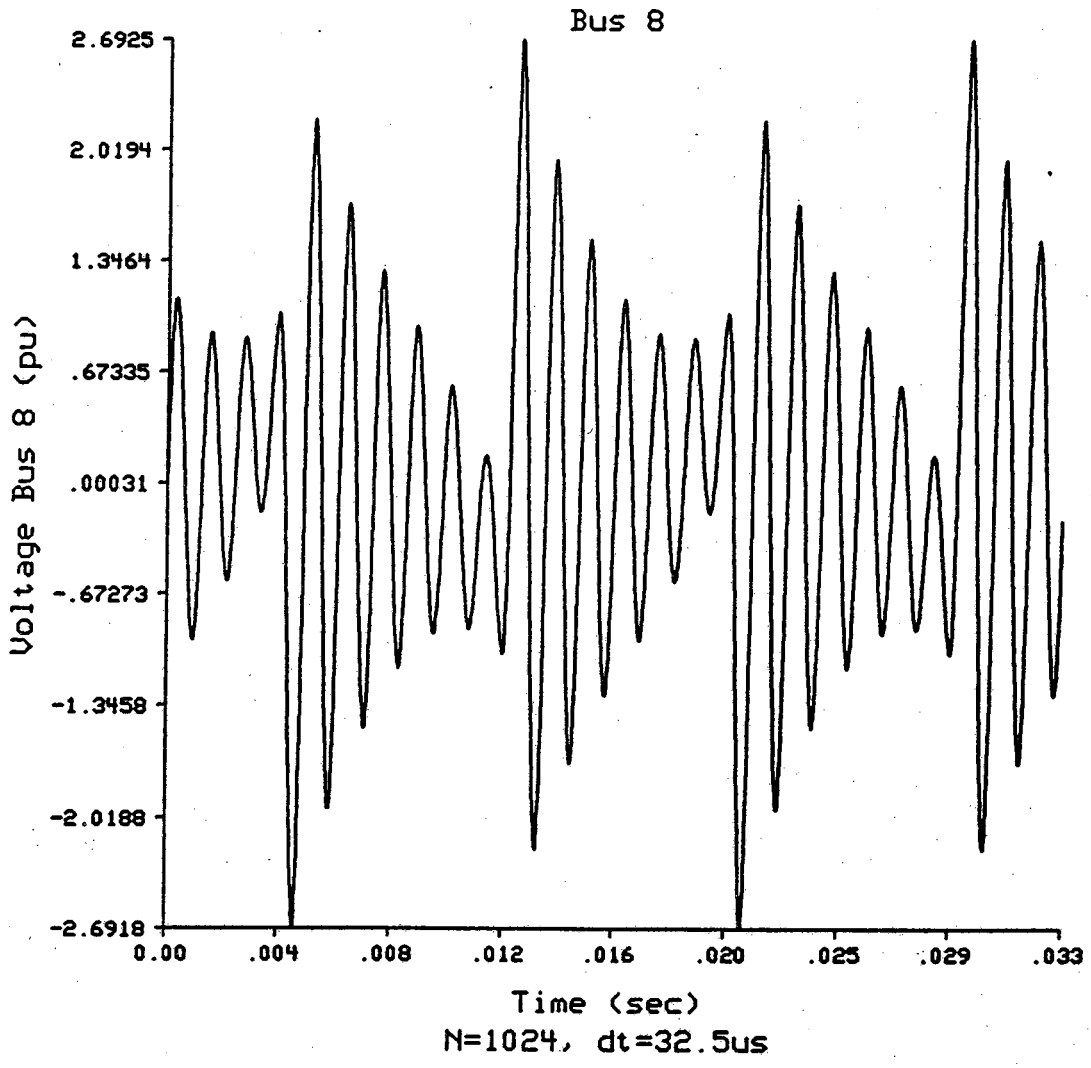

Figure 3.11 Fourier transform solution of steady state voltage at bus 8 due to current in Figure 3.9.

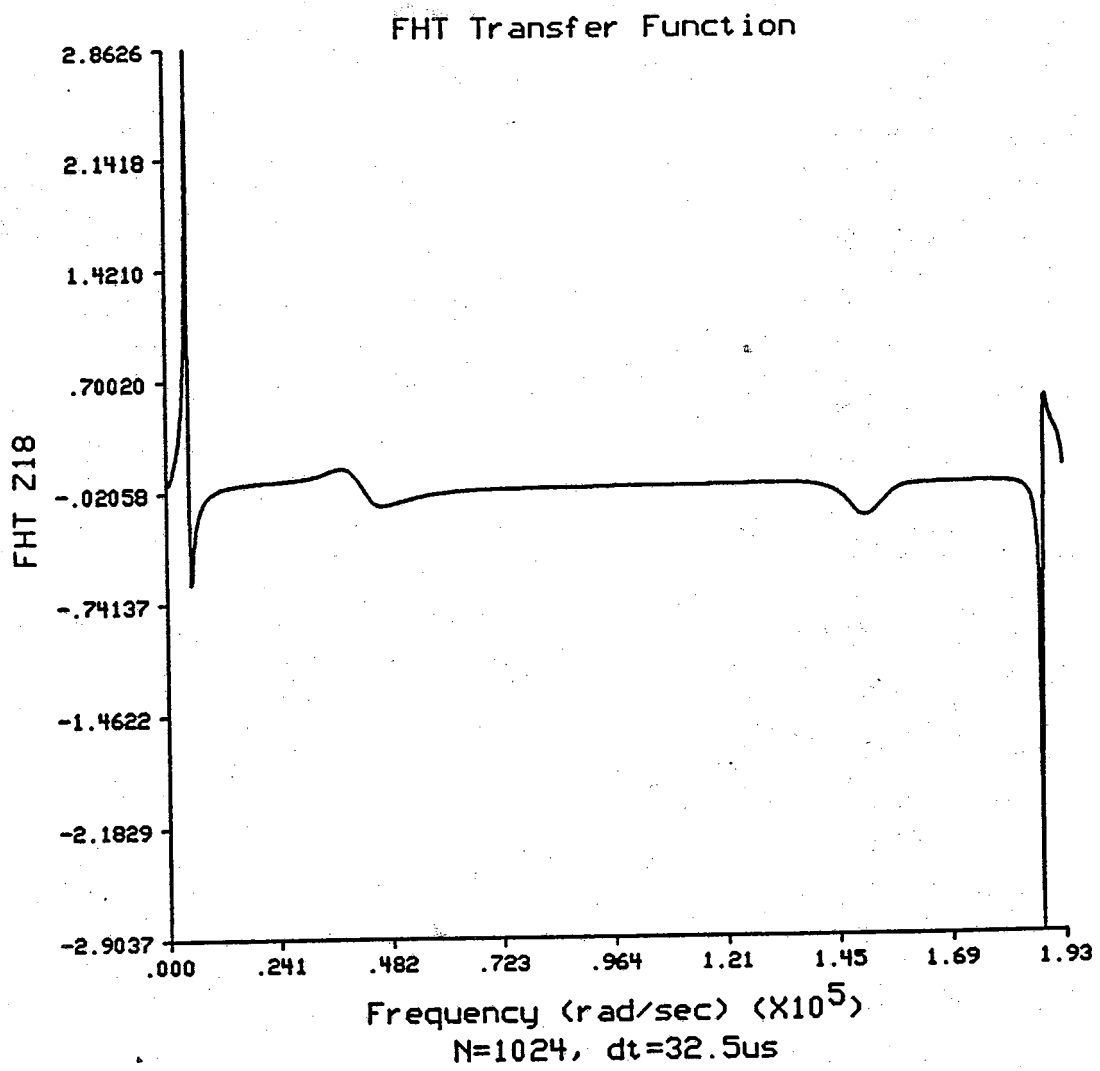

Figure 3.12 Hartley transform representation of frequency spectrum of transfer impedance $Z_{1,8}$.

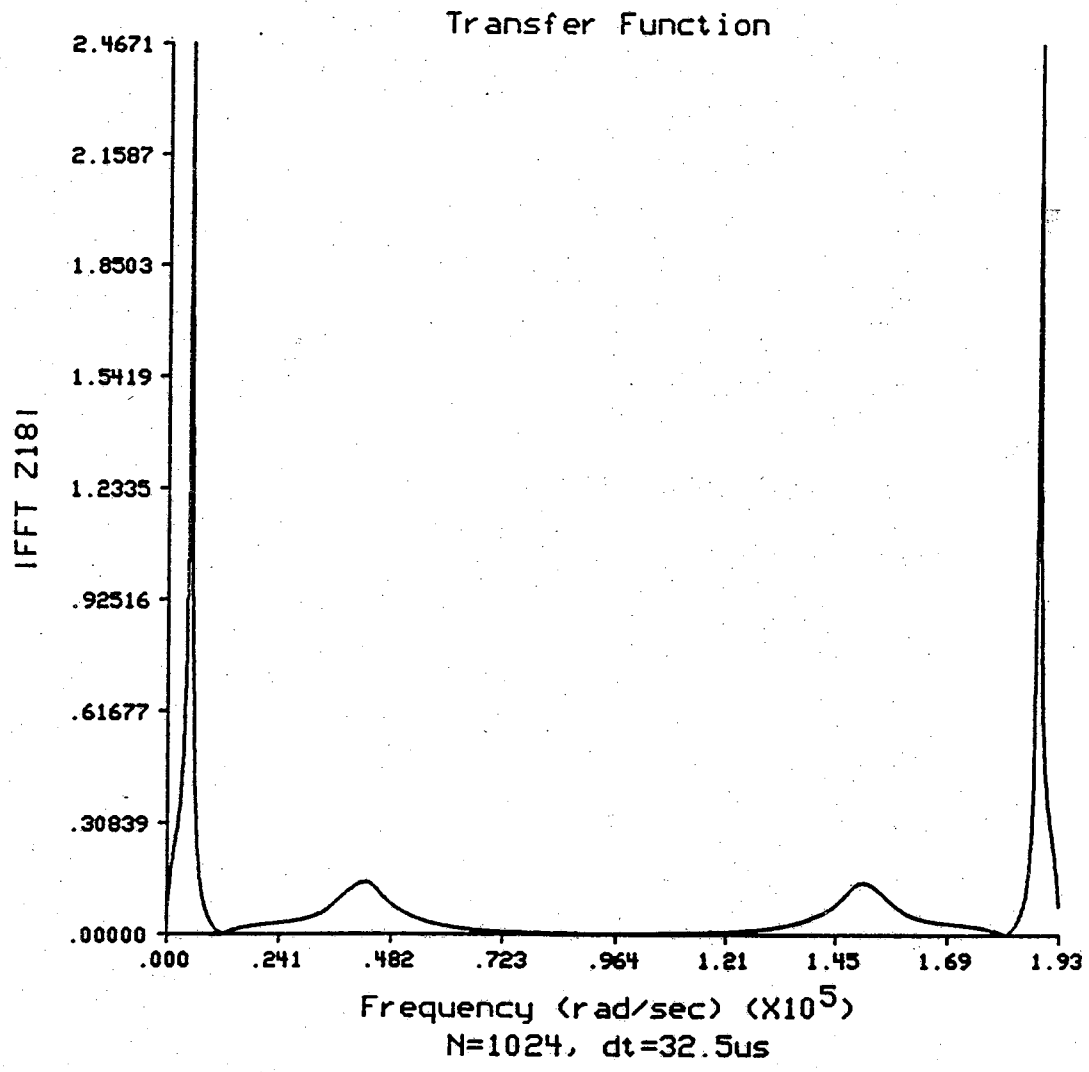

Figure 3.13 Magnitude of Fourier transform representation of frequency spectrum of transfer impedance $Z_{1,8}$. Resonant frequency is at 4900 rad/sec.

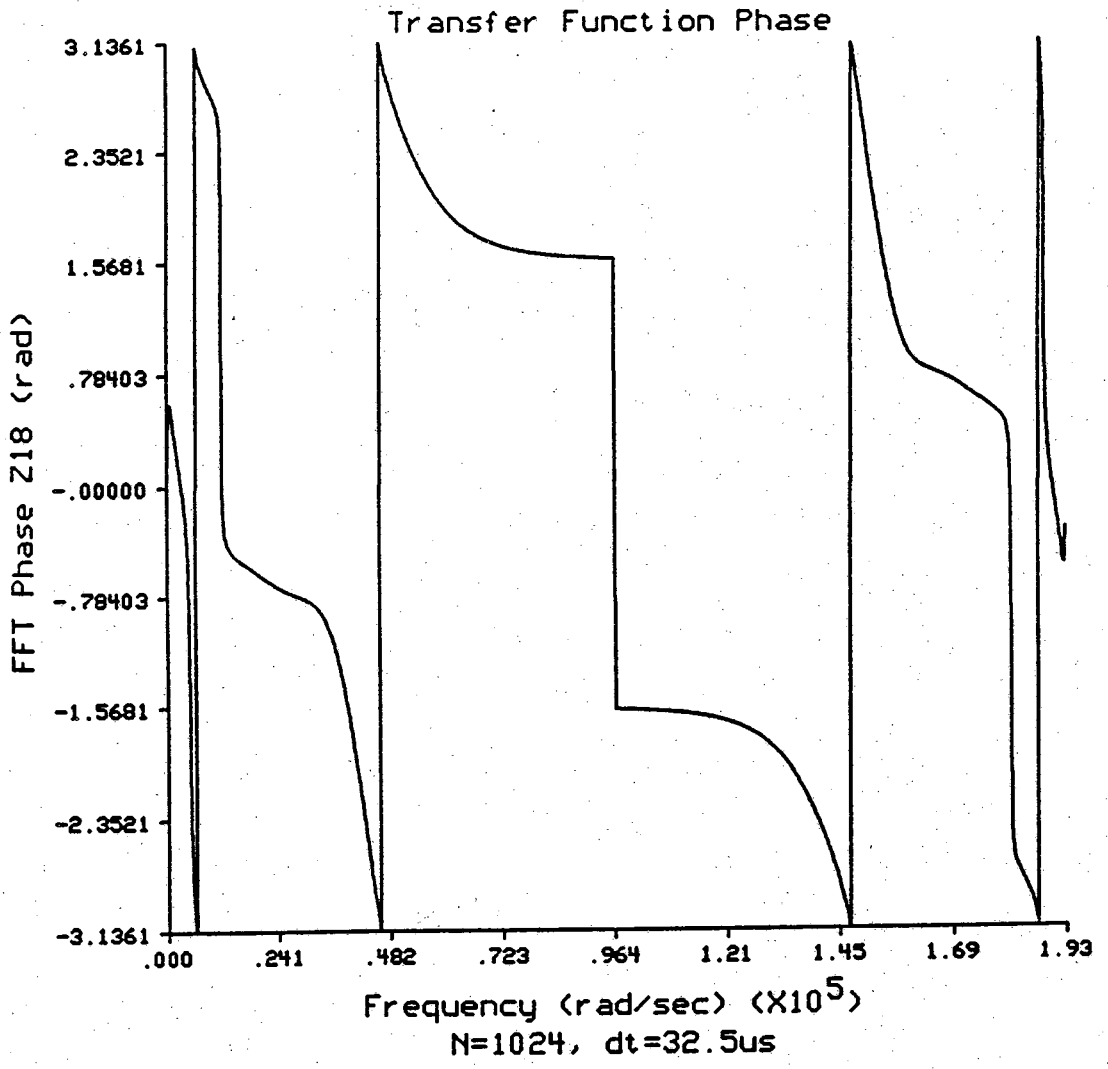

Figure 3.14 Phase of Fourier transform representation of transfer impedance $Z_{1,8}$.

Δt — resolution of the time samples

Ω — resolution of the frequency samples

N — total number of samples.

The relationships between the parameters allow only two of them to be chosen and the other three are calculated from the two chosen.

Additionally, the methods described here impose more constraints:

- $t_f = nT$, where T = period of the injected current in seconds, and $n = 0,1,2,...$
- The number of samples of the transfer function and the injected current must be equal.
- The resolution of the frequency samples of the transfer function and the injected current must be equal.

Figure 3.15 shows the discrete Fourier transform representation of the current which was injected into the eight bus system. Clearly, the choice of Ω_{max} = 96.5 krad/sec introduces a negligible amount of aliasing error on the frequency samples of the injection current. In fact, in order to reduce the number of computations, Ω_{max} can be reduced significantly and the calculated bus voltages will still be accurate. The choice of Ω_{max} = 96.5 krad/sec corresponds to the sampling rate $\Delta t = 32.5$ μs. Table 3.1 shows some other choices of sampling parameters which were used to calculate the bus voltages. For comparison, the maximum voltage calculated at bus one is listed in the last column for each choice of parameters. Comparing the maximum voltage obtained when $\Delta t = 32.5$ μs, and $\Delta t = 16.25$ μs shows that the aliasing error for the slower sampling rate is very small. Depending on the accuracy required, the calculation of only 64 points will provide a fairly accurate solution for the bus voltages. Note that Ω_{max} in Figure 3.15 can be reduced well below the 96.5 krad/sec shown in that graph. It appears that Ω_{max} can be reduced below the small lobe located at about 15.0 krad/sec. Table 3.1 bears out this remark, and one concludes that solutions with small N are indeed reasonably accurate.

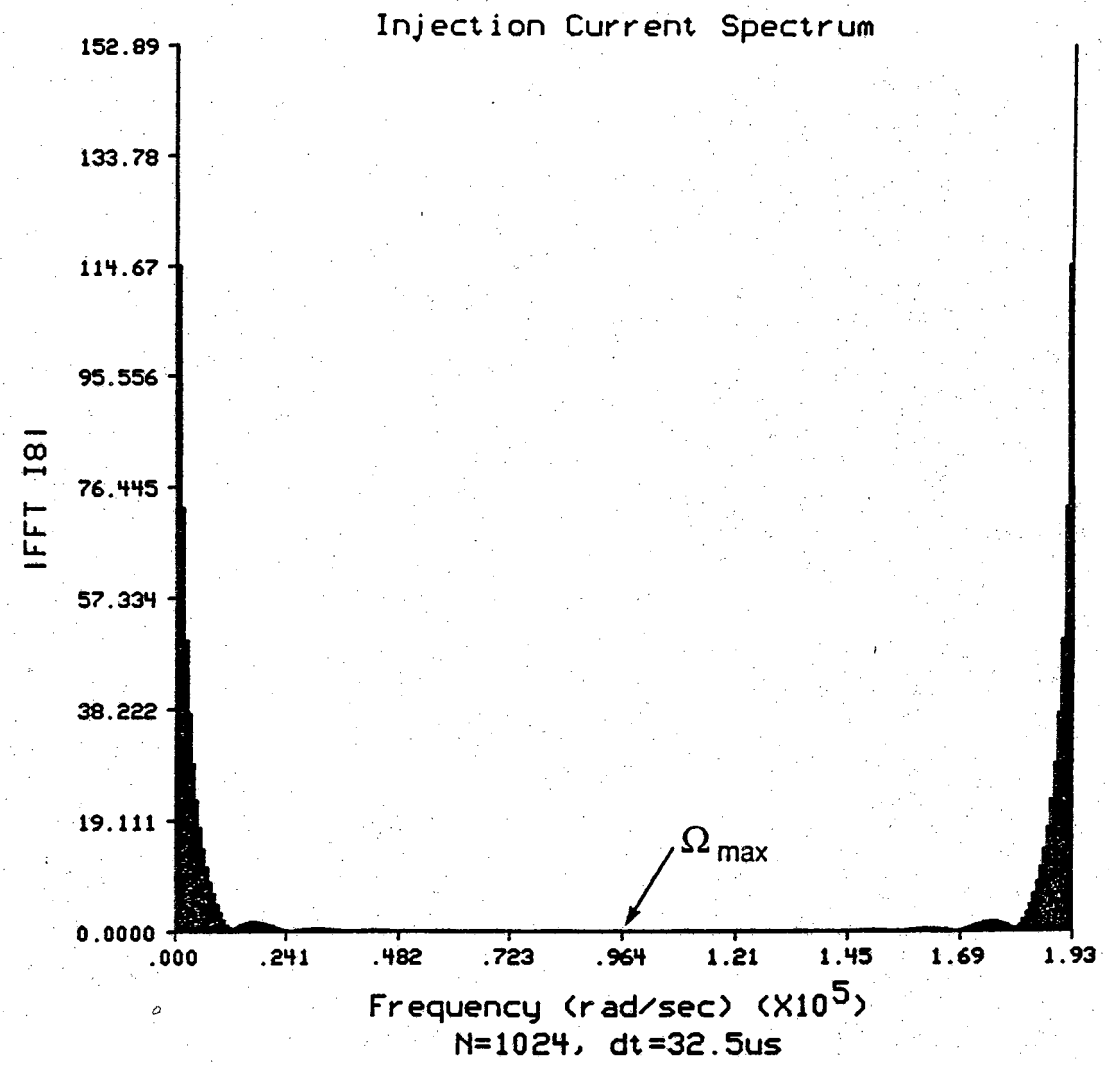

Figure 3.15 Magnitude of frequency spectrum of current shown in Figure 3.9, Fourier representation.

Table 3.1. Alternative choices of sampling parameters.

t_f	N	Ω_{max}	Δt	Ω	Max Voltage
$\frac{J}{60}$ $J = 1,2,...$	2^m $m = 1,2,...$	$\frac{\pi N}{t_f} = \frac{\pi}{\Delta t}$	$\frac{t_f}{N}$	$\frac{2\Omega_{max}}{N} = \frac{2\pi}{t_f}$	v_1
sec		rad/sec$\times 10^3$	μs	rad/sec	(pu)
8/60	8190	193.0	16.25	47.12	0.27382
8/60	4096	96.5	32.5	47.12	0.27397
2/60	1024	96.5	32.5	188.5	0.27397
1/60	512	96.5	32.5	377	0.27397
2/60	512	48.25	65.1	188.5	0.27473
1/60	256	48.25	65.1	377	0.27473
1/60	128	24.12	130.2	377	0.27889
1/60	64	12.6	260.4	377	0.26717
1/60	32	6.3	520.8	377	0.35777

CHAPTER IV
POWER SYSTEM REPRESENTATION

4.1 Modeling of the Network Components

Transmission lines

Under balanced conditions, a three phase transmission line can be represented by its single phase positive sequence nominal pi equivalent circuit. For long lines, a sequence of cascaded pi models can be used to approximate transmission line standing wave effects. Alternatively, long transmission lines can be represented by an equivalent pi model obtained from the solution of the well known second order differential equations obtained for transmission lines. The equivalent pi model is obtained by applying correction factors to the series impedance and shunt admittance [27], i.e.

$$\frac{\sinh\left(x\sqrt{Z'Y'}\right)}{x\sqrt{Z'Y'}} \quad \text{for the series impedance}$$

$$\frac{\tanh\left(x\sqrt{Z'Y'}/2\right)}{x\sqrt{Z'Y'}/2} \quad \text{for the shunt admittance} \qquad (4.1)$$

where x is the length of the line, $Z' = r + j\omega L$ is the series impedance per unit length, and $Y' = g + j\omega C$ is the shunt admittance per unit length. This model can be analyzed with the methods in Chapter II. Also, the frequency dependent skin effect phenomenon can be handled since the methods proposed here are discretized in the frequency domain. In short, calculations of frequency dependent parameters do not present difficulties.

Generators and transformers

Generators can be represented as a shunt impedance. Usually the subtransient reactance is used [27,28]. The Thevenin equivalent voltage should not be represented. This is the case since the power frequency signals are typically much larger than the nonsinusoidal signals which are to be analyzed. Also, there are numerous computationally efficient methods for calculating the power frequency voltages and currents (e.g. load flow studies). The power

frequency signals should be calculated separately and can be superimposed on the nonsinusoidal waveforms.

Assuming that the transformer is not operated in saturation, there are a number of frequency dependent linear models used. Some of these are described in [27-29]. When the transformer is saturated, the nonsinusoidal magnetizing current must be represented as a nonsinusoidal current injecting source.

Loads

For convenience, on a given feeder, individual loads are combined to form a composite equivalent. These equivalents can be as simple as a shunt impedance. There are also frequency dependent load models [27-30]. Nonlinear loads which produce nonsinusoidal demand currents are most commonly represented by ideal current sources. Reference [29] indicates that this method is adequate when the THD of the 60 Hz voltage is less than 10 percent.

Compensating capacitors and inductors are assumed to be pure elements with constant parameters.

Distribution systems can be isolated by representing the transmission system by its short circuit equivalent [29].

4.2 Sensitivity of Circuit Solution to Model Parameters and Injection Current Characteristics.

In this section the exemplary eight bus system in Figure 3.1 is revisited with the objective of illustrating the sensitivity of the solution to changes in the model parameters.

The voltage at bus 1 due to the original current injection in Figure 3.9 is shown in Figure 3.10. In order to illustrate the effects of varying the waveform i(t), the pulse current in Figure 4.1 is now injected. The voltage response is shown in Figure 4.2 Note that the maximum voltage 0.318 (pu) is larger than the maximum voltage of 0.274 (pu) in Figure 3.10. The resonant peak of the system is at 4900 rad/sec (see Figure 3.13). The frequency spectrums of the pulse current and the original current are shown if Figures 4.3 and 3.15 respectively. Comparing the two frequency spectrums shows that the pulse current contains more high frequency content than the original current. More importantly the pulse contains more current at 4900 rad/sec than the original waveform. This is why the voltage response is largest for the pulse current.

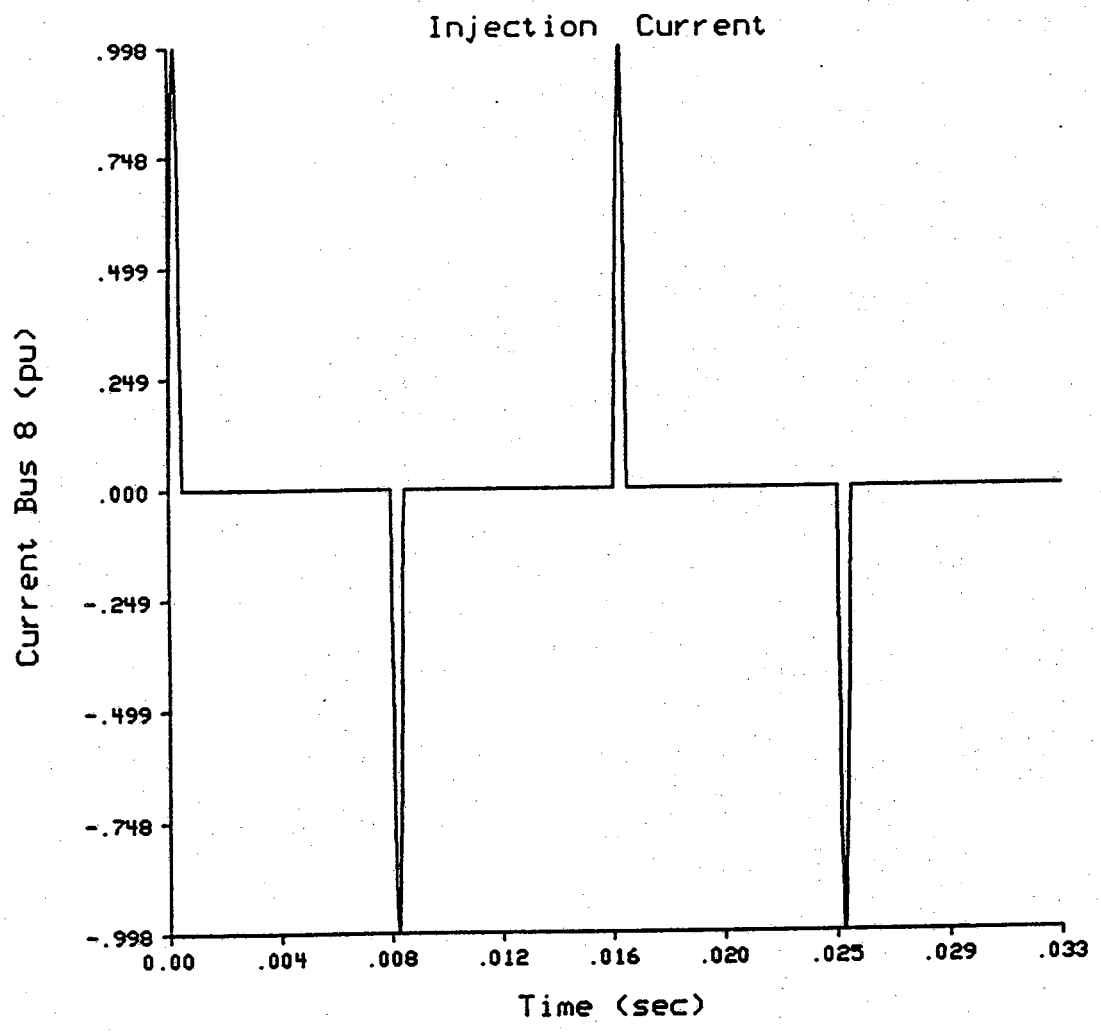

Figure 4.1 Injection current with high frequency characteristics due to short duration of pulses, injected into bus 8.

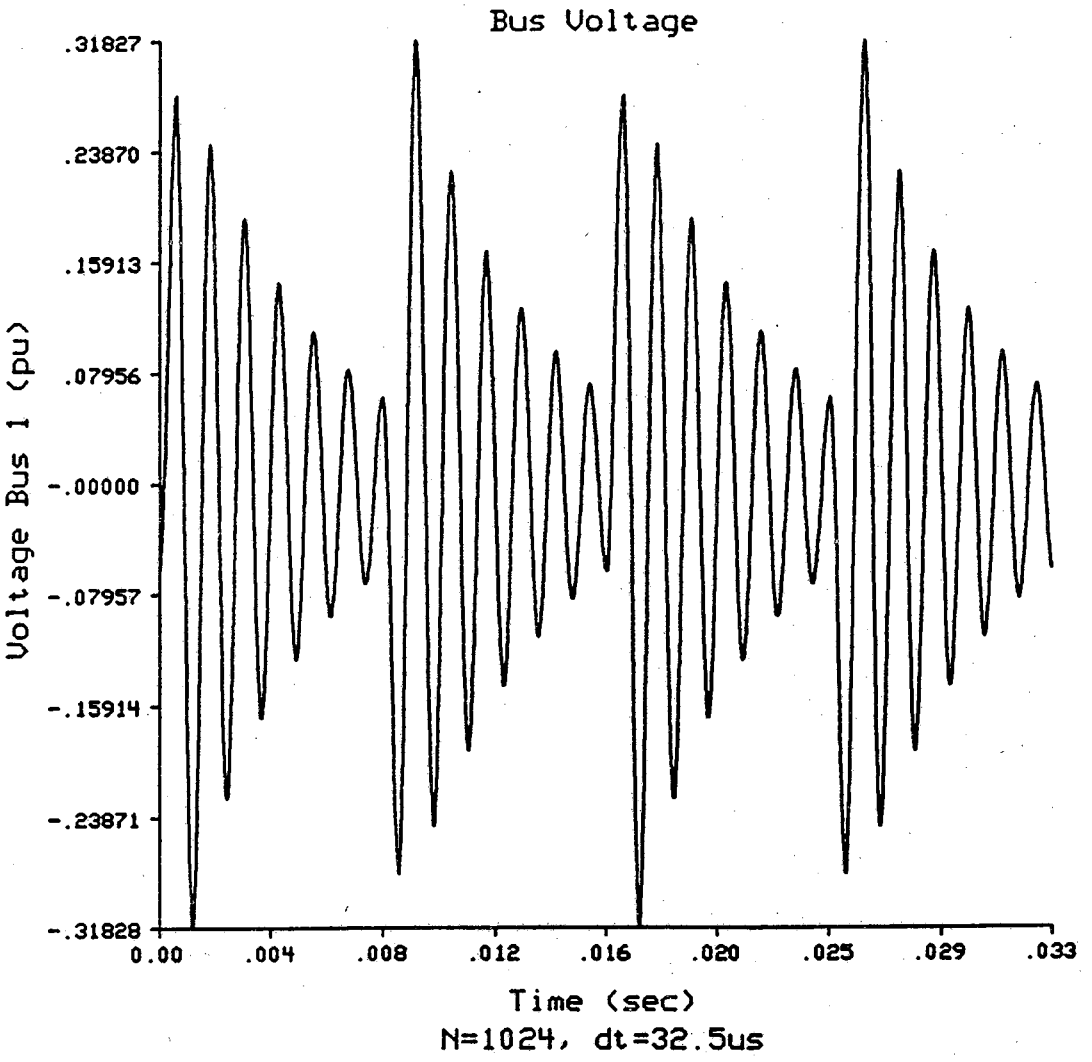

Figure 4.2 Voltage response at bus 1 due to pulse current in Figure 4.1.

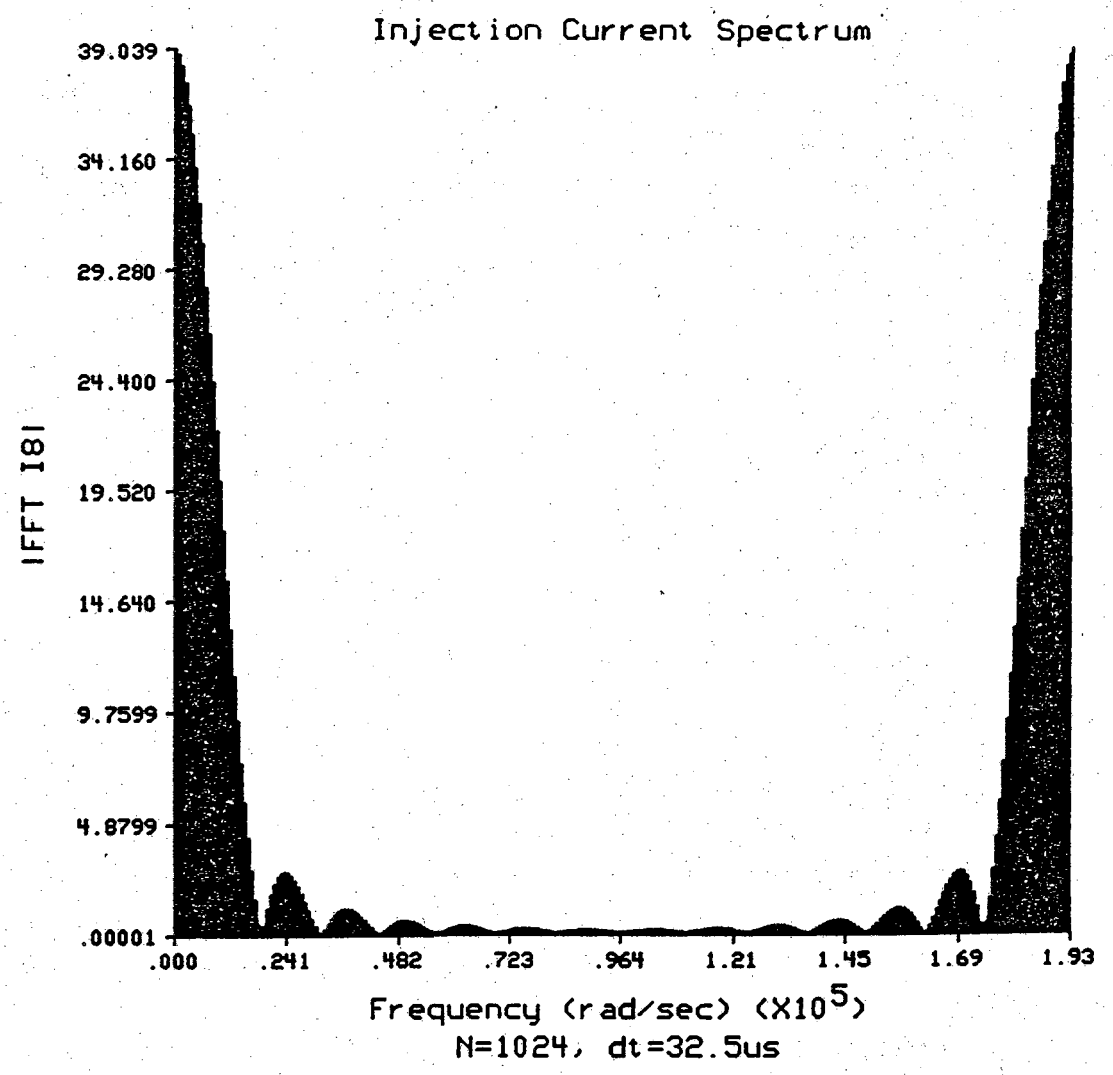

Figure 4.3 Magnitude of frequency spectrum of pulse current in Figure 4.1.

The line impedance for each of the transmission lines in Figure 3.1 is 0.001 + j 0.01. (pu) Each line impedance has been increased by ten to the value of 0.01 + j 0.1 (pu). This change had the effect of shifting back the resonant frequency about 377 rad/sec to 4523 rad/sec on the transfer function between buses 1 and 8 (Figure 4.4). The magnitude of the resonant peak also decreased from 2.46 (pu) to 2.28 (pu). This decrease in the transfer function between buses 1 and 8 resulted in a slower frequency and smaller magnitude voltage at bus one. Figure 4.5 shows the voltage at bus 1 for the new system. Note that, the current in Figure 3.9 is used in this and the remaining studies. The peak voltage of 0.199 (pu) is considerably smaller than the value of 0.274 (pu) for the original system. Another effect of the increased line impedances is an increased voltage difference between the buses. In the original system the voltage difference between buses 1 and 3 was 0.025 (pu). This modified system had a voltage difference between buses 1 and 3 of 0.046 (pu).

The effect of decreasing the transformer impedance of the original system is now studied. The series impedance of the transformer was changed from 0.01 + j 0.1 (pu) to 0.005 + j 0.05 (pu). The effect of changing the transformer impedance shifted the resonant frequency up 1074 rad/sec to 6974 rad/sec. The magnitude of the resonant peak decreased from 2.46 (pu) to 1.94 (pu) for the transfer function between buses 1 and 8 (Figure 4.6). The resulting voltage at bus 1 for this modified system is shown in Figure 4.7. The peak value of the voltage of 0.209 (pu) is lower than 0.274 (pu) for the original system.

The effect of reducing the equivalent impedance of the external system is now examined. The equivalent impedance was reduced from 0.1 + j 0.1 (pu) to 0.01 + j 0.01 (pu). This change shifted the resonant frequency back only 188 rad/sec. The transfer function in Figure 4.8 is for the modified system, and Figure 3.13 is the transfer function for the original system. Note that the transfer function of the modified system for frequencies below the resonant frequency has been practically eliminated compared to the original system. Most of the injection current spectrum is below the resonant frequency. Therefore one would expect a significant drop in the voltage at bus 1 for this modified system compared to the original system. Figure 4.9 shows the voltage at bus 1 for the modified system, and the peak voltage has been reduced to almost a third of the original system voltage.

Finally the effect of increasing the shunt capacitors in Figure 3.1 was studied. All of the shunt capacitors in the system were increased by a factor of ten. Figure 4.10 shows the transfer function between buses 1 and 8 for this modified system. The resonant peak has been reduced 3204 rad/sec to 1696 rad/sec. With the resonant frequency shifted to coincide with the largest part

of the injection current spectrum one would expect a large voltage response at bus 1. Figure 4.11 shows the voltage at bus 1. However, the 0.192 (pu) peak value is less than the 0.274 (pu) for the original system. This value is smaller for two reasons. The magnitude of the resonant peak is 0.838 (pu) which is less than 2.46 (pu) for the original system. Also the modified system's time constants are slower and cannot follow the injection current waveform as closely as the original system.

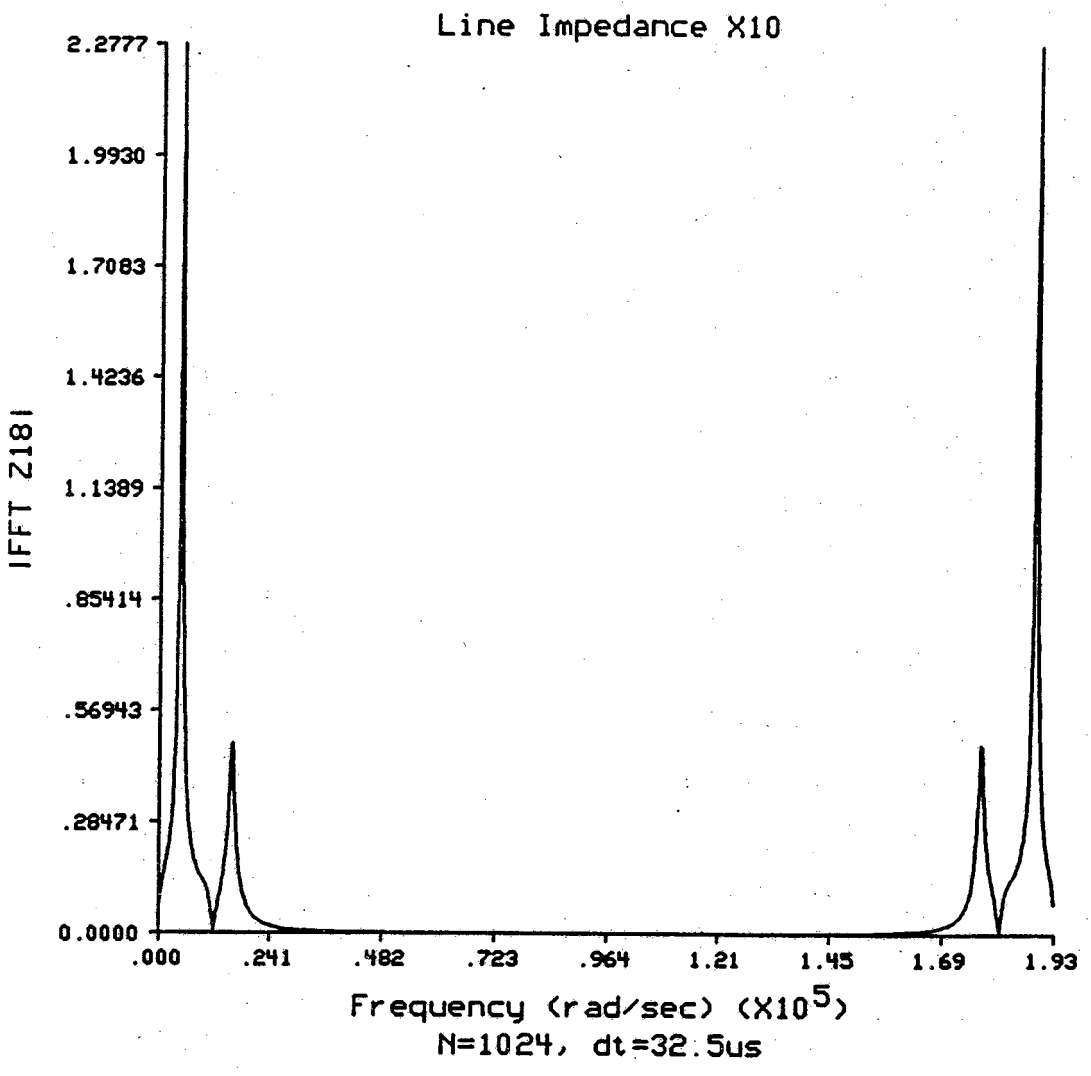

Figure 4.4 Magnitude of frequency spectrum of transfer impedance $Z_{1,8}$. All transmission line impedances have been increased to 0.01 + j 0.1 (pu). Resonant frequency is at 4523 rad/sec.

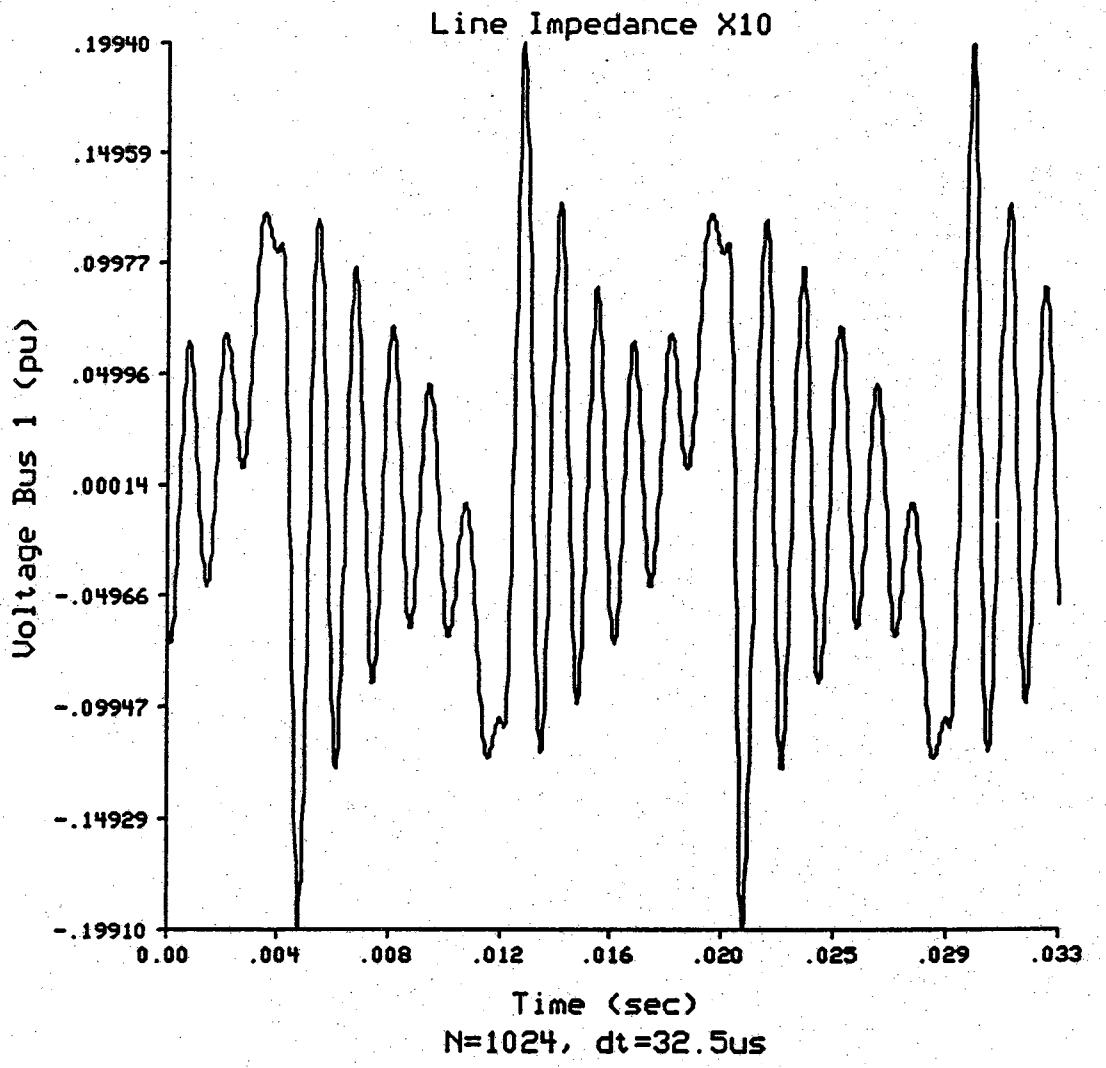

Figure 4.5 Voltage at bus 1 due to current in Figure 3.9. All transmission line impedances have been increased to 0.01 + j 0.1 (pu).

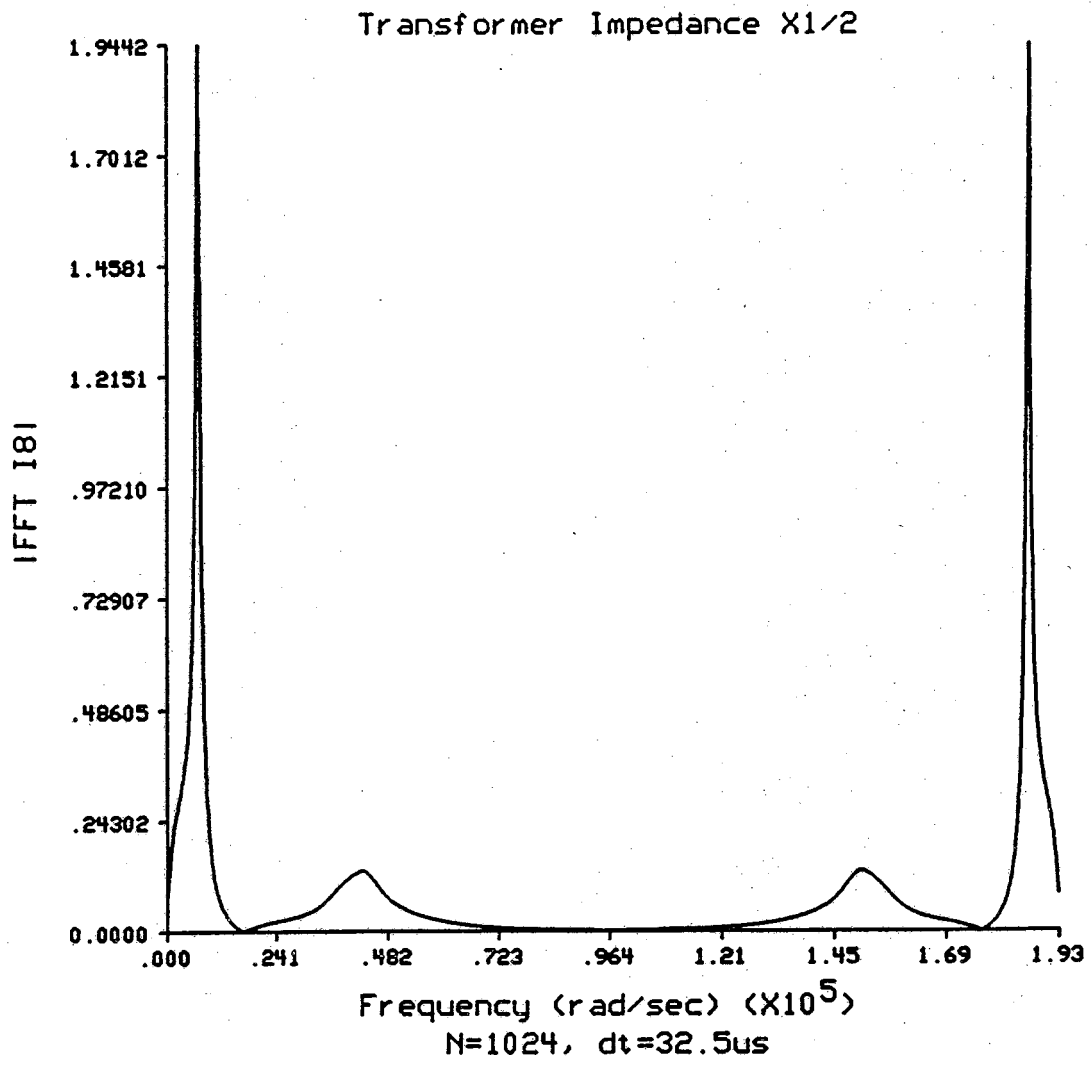

Figure 4.6 Magnitude of frequency spectrum of transfer impedance $Z_{1,8}$. Transformer series impedance has been changed to 0.005 + j 0.05 (pu). Resonant frequency is at 6974 rad/sec.

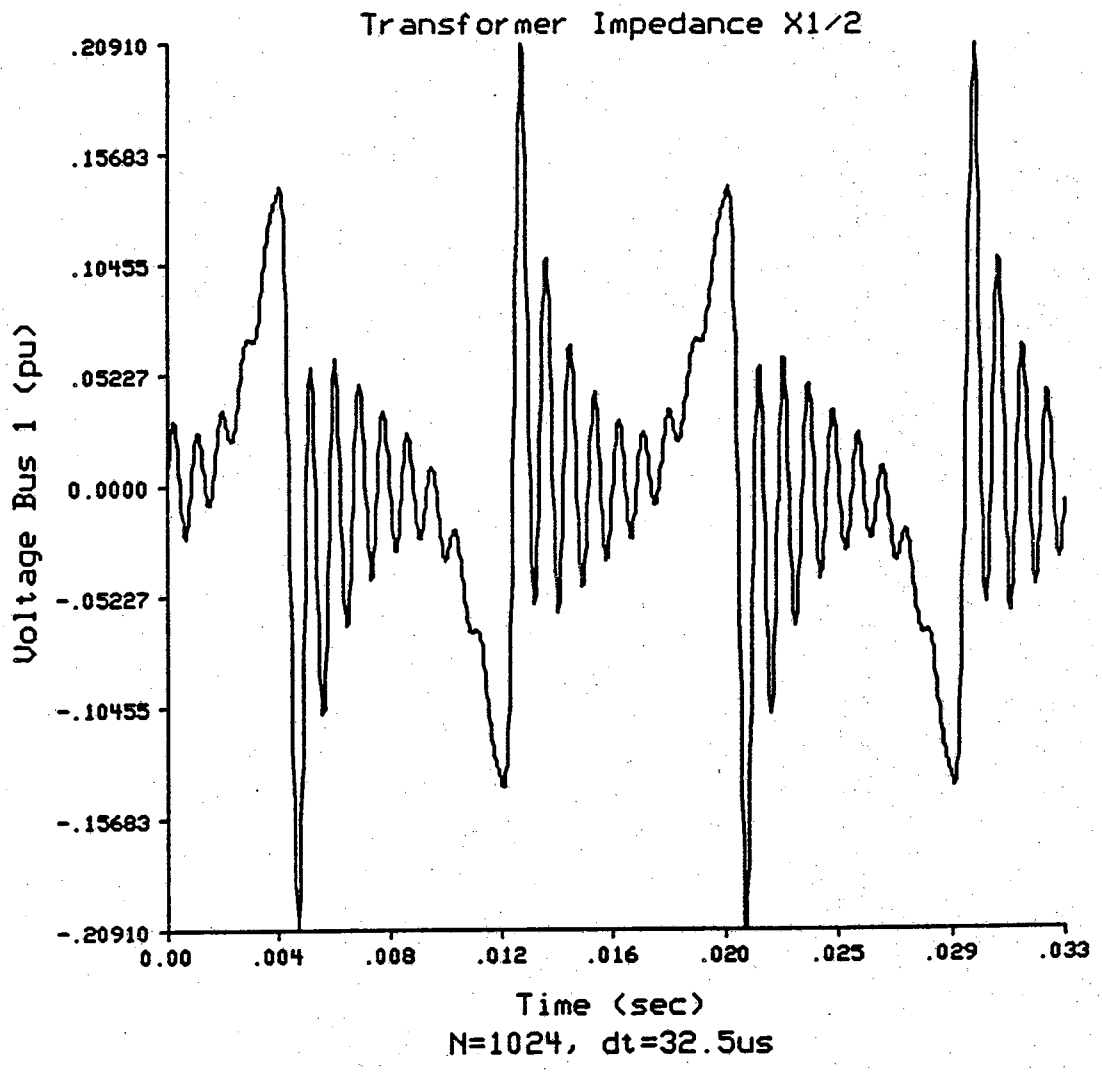

Figure 4.7 Voltage at bus 1 due to current in Figure 3.9. Transformer series impedance has been changed to 0.005 + j 0.05 (pu).

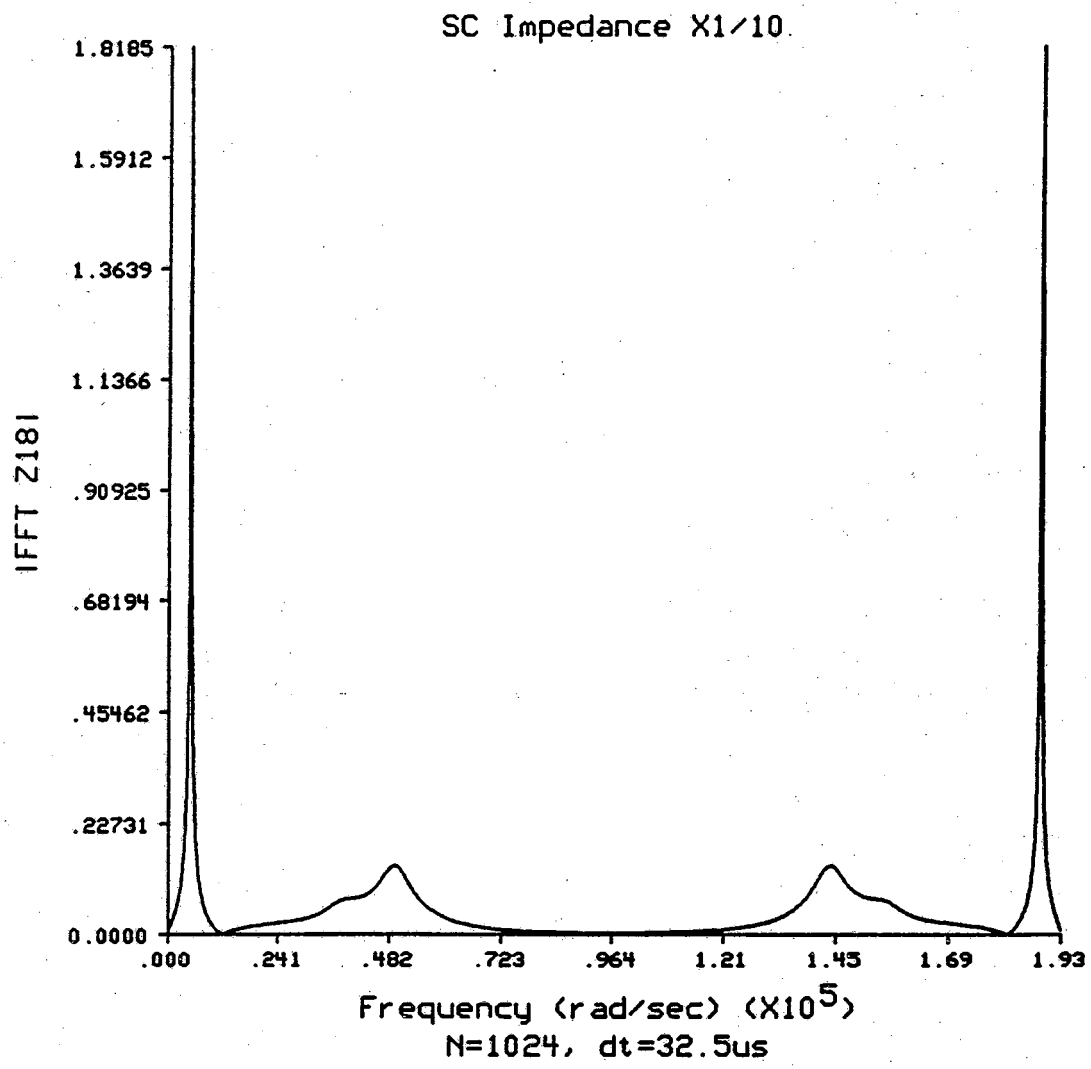

Figure 4.8 Magnitude of frequency spectrum of transfer impedance $Z_{1,8}$. External system equivalent impedance has been changed to 0.01 + j 0.01 (pu). Resonant frequency is at 4712 rad/sec.

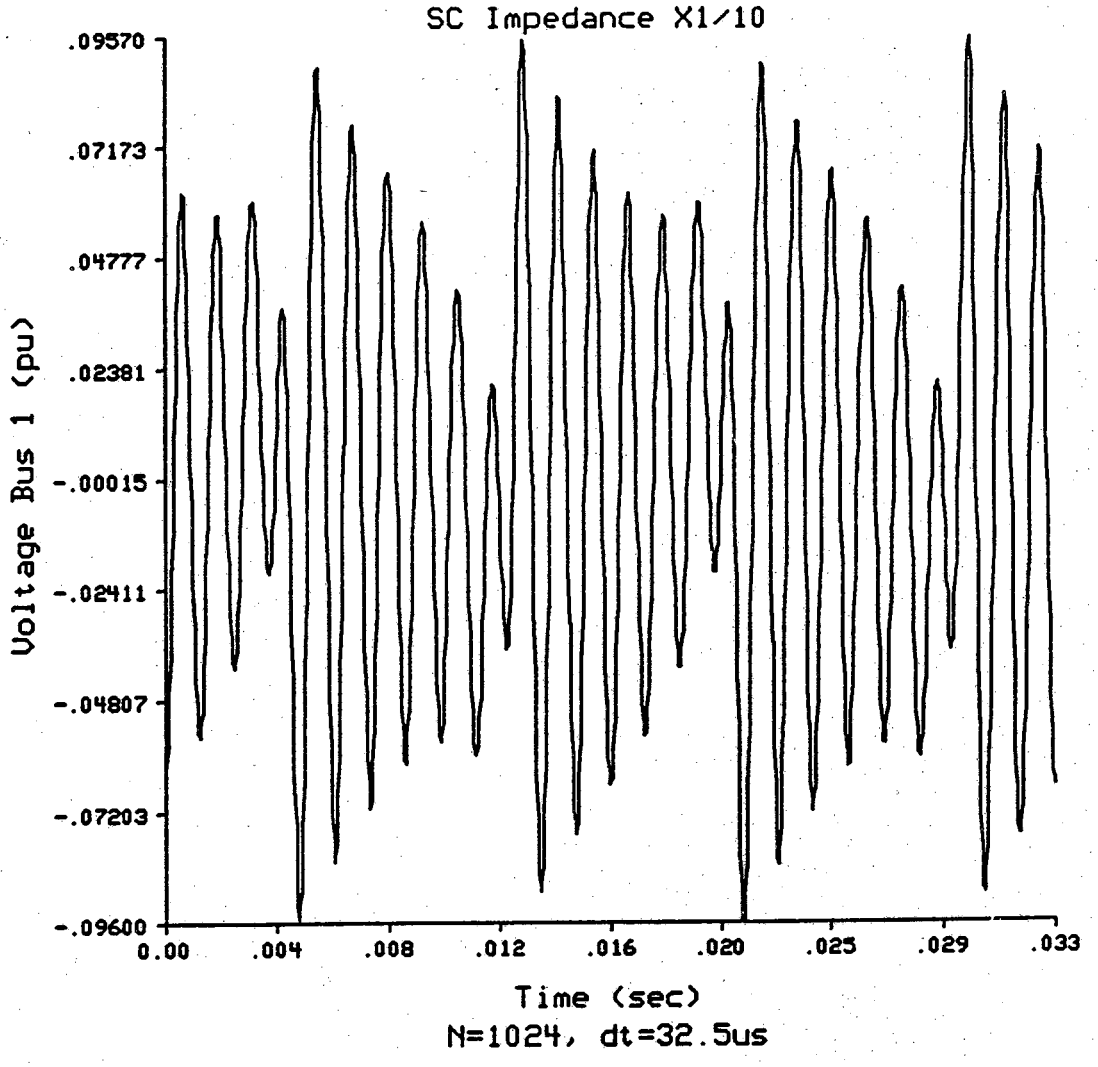

Figure 4.9 Voltage at bus 1 due to current in Figure 3.9. External system equivalent impedance has been changed to 0.01 + j 0.01 (pu).

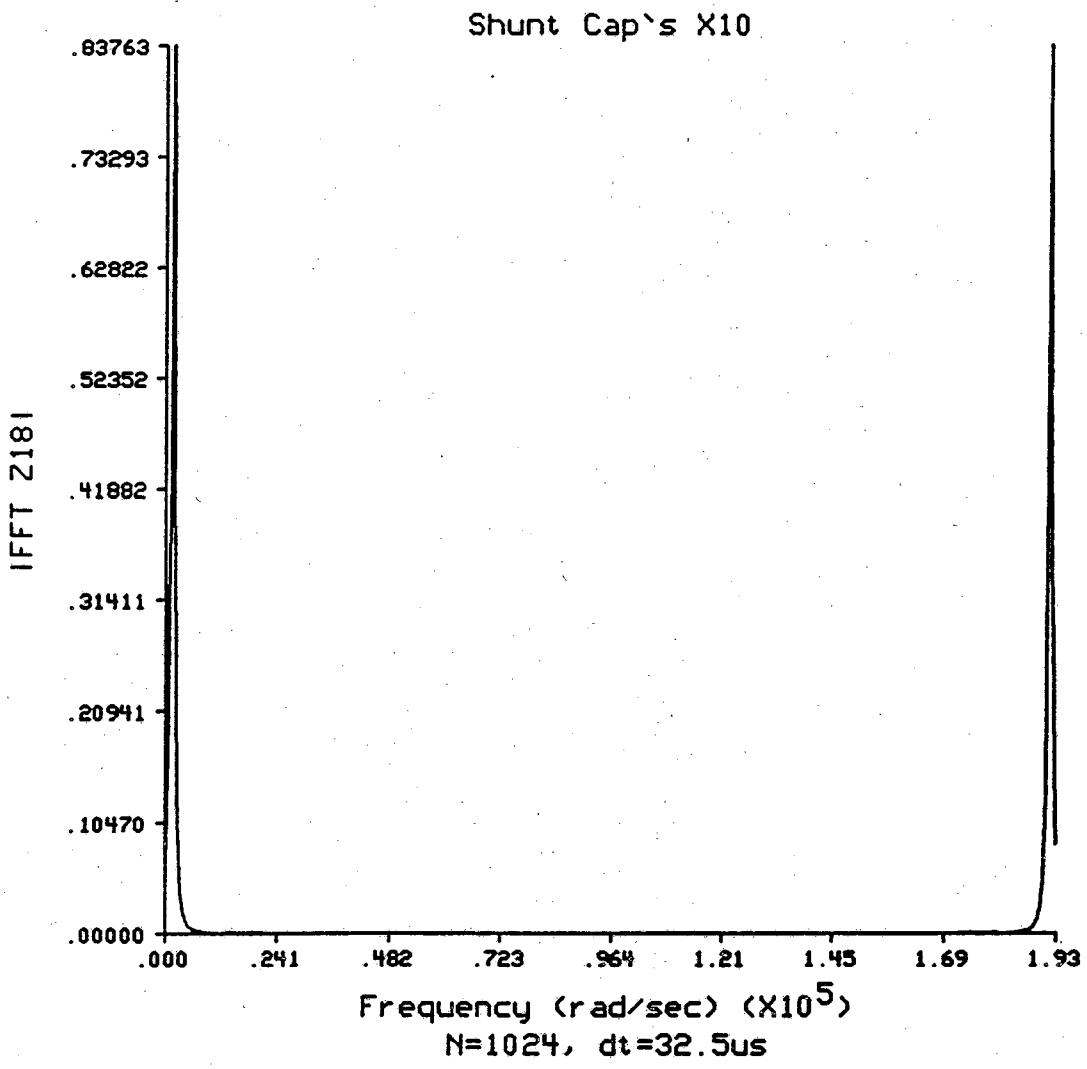

Figure 4.10 Magnitude of frequency spectrum of transfer impedance $Z_{1,8}$. All shunt capacitances have been increased by a factor of 10. Resonant frequency is at 1696 rad/sec.

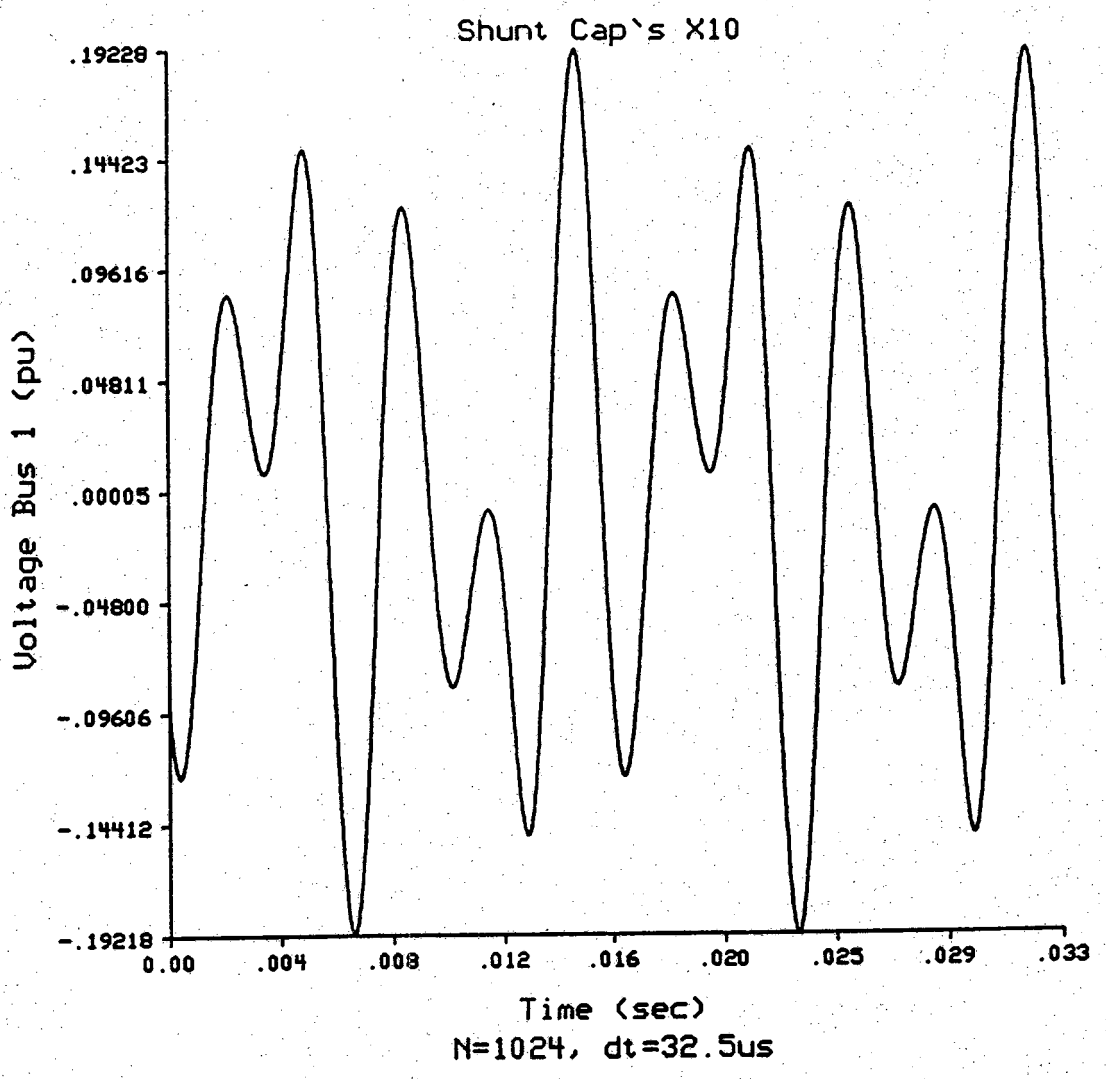

Figure 4.11 Voltage at bus 1 due to current in Figure 3.9. All shunt capacitances have been increased by a factor of 10.

CHAPTER V
CONCLUSIONS AND RECOMMENDATIONS

The node voltages of an example power system due to a nonsinusoidal demand current were calculated. Three different frequency domain methods were used to solve the problem: Laplace transform, Fourier transform, and Hartley transform. The results were checked by solving the problem with the time domain simulation routine SPICE. The Laplace transform solution method used an iterative inverse Laplace transform routine and required 166 seconds on a Gould NP1 to calculate the 150 points plotted in Figure 3.3. The Fourier and Hartley solution methods used fast algorithms available to calculate their respected discrete transforms The 1024 time samples of the bus voltage calculated, for both methods, took less than 5 seconds to compute. Because the majority of that time was dedicated to operations other than frequency transformations, the advantage of the Hartley transform over the Fourier transform was not well illustrated. For large systems, long simulation times, and cases of significant high frequency phenomena, the Hartley transform gains a computational advantage. As a comparison to a time domain simulation routine the SPICE program required 131 seconds to calculate the 1700 points shown in Figure 3.6. Clearly, the fast Fourier transform and fast Hartley transform were the superior methods. For circuit solutions with very large computational burden, one would continue to expect to gain a computational advantage of one to two orders of magnitude over a SPICE solution using the fast Fourier and Hartley transforms. Also, for problems with high computational burden, one would expect to approach the theoretical computational advantage of two for the fast Hartley transform over the FFT. This advantage occurs due to the use of real numbers in the Hartley domain as compared to complex numbers in the Fourier domain.

The majority of the computation time spent by the Fourier and Hartley transform methods is on the inversion of the matrix Y_{bus} to compute Z_{bus}. Reference [31] proposes a method of estimating Z_{bus} which does not require matrix inversions. Extensive work in developing this theory would greatly improve the methods introduced in this thesis. In addition employing these frequency domain methods on power system data taken from existing power

systems is recommended. This would allow further development of more accurate system models. In addition, guidelines could be developed for initial choices of sampling parameters.

A further recommendation is that alternative transforms should be studied for applicability of nonsinusoidal waveform propagation studies. Real transforms offer computational advantages which should be investigated.

Finally, the examples shown in this thesis indicate that it is possible to obtain reasonable solution occuracy with considerable speed by reducing the number of points in FFT and fast Hartley solutions. Further reductions in the number of points should be considered. Methods to retain accuracy with reduced values of N should be studied.

LIST OF REFERENCES

LIST OF REFERENCES

[1] R. N. Bracewell, "The Fourier Transform and Its Applications," McGraw-Hill, NY, 1986.

[2] J. S. Walker, "Fourier Analysis," Oxford University Press, NY, 1988.

[3] I. H. Sneddon, "The Use of Integral Transforms," McGraw Hill, NY, 1972.

[4] M. C. Potter, J. Goldberg, "Mathmatical Methods," 2nd ed., Prentice Hall, Englewood Cliffs, NJ, 1987.

[5] T. B. Senior, "Mathematical Methods used in Electrical Engineering," Cambridge Univ. Press, NY, 1986.

[6] K. S. Krump, "Numerical Inversion of Laplace Transforms Using a Fourier Serier Approximation," Journal of the Assoc. for Comp. Mach., Vol. 23, No. 1, pp. 89-96, January 1976.

[7] R. Piessens, R. Huysman, "Automatic Numerical Inversion of the Laplace Transform," ACM Trans. on Mathematical Software, Vol. 10, No. 3, pp. 348-353, September 1984.

[8] B. Barbow, G. Giunta, J. Lyness, "Software for an Implementation of Weeks Method for the Inverse Laplace Transform," ACM Transactions on Mathematical Software, Vol. 14, No. 2, pp. 163-170, June 1988.

[9] A. Papoulis, "Circuits and Systems A Modern Approach,"; Holt, Rhinehart and Winston, Inc., NY, 1980.

[10] C. McGillem, G. Cooper, "Continuous and Discrete Signal and System Analysis," 2nd ed.; Holt, Rhinehart and Winston, NY, 1984.

[11] R. V. L. Hartley, "A More Symmetrical Fourier Analysis Applied to Transmission Problems," Proc. Institute of Radio Engineers, Vol. 30, No. 3, pp. 144-150, March 1942.

[12] R. N. Bracewell, "The Hartley Transform," Oxford Univ. Press, NY, 1986.

[13] D. J. DeFatta, J. G. Lucas, W. S. Hodgkiss, "Digital Signal Processing," Wiley, NY, 1988.

[14] R. Sorensen, D. Jones, C. Burrus, M. Heideman, "On Computing the Descrete Hartley Transform," IEEE Trans. on Acoustics, Speech, and Signal Processing, Vol. ASSP-33, No. 4, pp. 1231-1238, October 1985.

[15] H. W. Dommel, W. S. Meyer, "Computation of Electromagnetic Transients," Proc. of IEEE, Vol. 62, No. 7, pp. 983-993, July 1974.

[16] R. C. Degeneff, "Reducing Storage and Saving Computational Time with a Generalization of the Dommel (BPA) Solution Method," IEEE PICA Conference, pp. 307-313, 1977.

[17] J. P. Bickford, N. Mullineux, J. R. Reed, "Computation of Power System Transients," Peter Peregrinus Ltd., England 1976.

[18] E. B. Makram, A. A. Girgis, "Electromagnetic Transients Due to Single Pole Tripping of a Faulted Long Transmission Line," Electric Power Systems Research, V. 13, No. 1, August, 1987, pp. 1-9.

[19] E. B. Makram, G. G. Koerber, K. C. Kruempel, "An Accurate Computer Method for Obtaining Boundary Conditions in Faulted Power Systems," IEEE Trans. on Power Apparatus and Systems, V. PAS-101, No. 9, September, 1982, pp. 3252-3260.

[20] M. F. McGranaghan, R. C. Dugan, J. A. King, W. T. Jewell, "Distribution Feeder Harmonic Study Methodology," IEEE 1984 T&D Conf.

[21] H. Skilling, "Electric Networks," Wiley, NY, 1974.

[22] W. Blume, "Computer Circuit Simulation," Byte, July 1986, pp. 165-170.

[23] G. T. Heydt, "Computer Analysis Methods for Power Systems," Macmillen, N.Y., 1986.

[24] James W. Nilsson, "Electric Circuits," Addison-Wesley, Reading MA, 1986.

[25] G. T. Heydt, K. J. Olejniczak, R. Sparks, E. Viscito, "Application of the Hartley Transform for the Analysis of the Propagation of Nonsinusoidal Waveforms in Power Systems," to be published.

[26] Paul Anderson, "Analysis of Faulted Power Systems," Iowa State Univ. Press, Ames, Iowa, 1973.

[27] J. Arrillaga, D. A. Bradley, P. S. Bodger, "Power System Harmonics," Wiley, NY, 1985.

[28] Aly A. Mahmoud, Richard D. Shultz, "A Method for Analyzing Harmonic Distribution in A.C. Power Systems," IEEE Trans. Pwr. App. and Syst., Vol. PAS-101, No. 6, June 1982.

[29] M. F. McGranaghan, R. C. Dugan, W. L. Sponsler, "Digital Simulation of Distribution System Frequency-Response Characteristics," IEEE Trans. Power Apparatus and Systems, Vol. PAS-100, No. 3, March 1981.

[30] D. J. Pileggi, N. Harish Chandra, A. E. Emanuel, "Prediction of Harmonic Voltages in Distribution Systems," IEEE Trans. Power Apparatus and Systems, Vol. PAS-100, No. 3, March 1981.

[31] G. T. Heydt, "A New Method for the Calculation of Subtransmission and Distribution System Transients Based on the FFT," IEEE Winter Power Meeting, Jan. 27 - Feb. 2 1989, New York.

APPENDIX

APPENDIX

A listing of the program that was used to calculate the bus voltages using the fast Hartley transform follows. The program using the fast Fourier transform is similar except that the transform subroutine, and convolution formula used are different. In order to analyze a new system, new Laplace domain equivalents for Y_{bus} can be coded into the complex function F. In order to analyze a different current injection, new expressions can be coded into the function CURR.

```
c*************************************************************
c
c     Main Program
c
c     Calculates bus voltages due to
c     nonsinusoidal currents
c
c*************************************************************
      program fhtmeth
      parameter (np = 1024)
      complex a(np),omega,f,y(8,8)
      real h1(np),e(np),hv(np)
      m = 10
      tf = 2./60.
      dt = tf/np
      np2 = np/2
c
c-----Calculate Zbus-------------------------------------
c
      do 38 i=1,8
      do 39 j=1,8
      y(i,j) = cmplx(0.,0.)
   39 continue
   38 continue
c
      do 10 ni = 1,np2
      n = ni - 1
      freq = n/tf
      w = 8.*atan(1.) * freq
      omega = cmplx(0.,w)
      a(ni) =  f(omega,y)
   10 continue
c
      a(np2+1)=cmplx(0.,0.)
      do 20 ni = np2 + 2,np
      nc = np - ni + 2
      a(ni) = conjg(a(nc))
   20 continue
c
c-----Calculate Injection Current Spectrum----------------
c
      do 40  i = 1,np
      t2 = (i - 1) * dt
      e(i) = curr(t2)
   40 continue
      call fht2t(e,np,m)
c
c ----Hartley Convolution--------------------------------
c
      do 130 i = 1,np
      h1(i) = real(a(i)) - aimag(a(i))
  130 continue
      hv(1) = (h1(1)*e(1))
      do 132 i=2,np
```

```
      hv(i) = .5*(h1(i)*e(i) - h1(np-i+2)*e(np-i+2) +
     2h1(i)*e(np-i+2) + h1(np-i+2)*e(i))
  132 continue
c
c-----Inverse Hartley Transform-----------------------------
c
      call fht2t(hv,np,m)
c
      open (9,file='time')
      open (8,file='v1')
c
      do 30  i = 1,np
      t = (i - 1) * dt
c
      write(9,240)t
      write(8,240)hv(i)/(np)
  30  continue
c
  240 format (f12.6)
      stop
      end
c*****************************************************************
c      Complex Function F
*****************************************************************
      complex function f(s,y)
      complex s,y(8,8),z(8,8),d456,ym
      y(1,4)=-1./(.001+26.5e-6*s)
      y(4,1)=y(1,4)
      y(1,6)=y(1,4)
      y(6,1)=y(1,4)
      y(1,1)=1./(.1+265e-6*s) + s/18.8e3 - y(1,4) - y(1,4)
c
      y(2,2)=s/18.8e3 + 1. - y(1,4) - y(1,4)
      y(2,3)=y(1,4)
      y(3,2)=y(1,4)
      y(2,6)=y(1,4)
      y(6,2)=y(1,4)
c
      y(3,3)=s/37.7e3 + .5 - y(1,4)
c
      d456 = (6.95228e-10)*(s**2) + (5.3e-8)*s + 1.e-6
      ym = -(2.65e-6)*s/d456
c
      y(4,5)=-(.001 + (26.5e-6)*s)/d456
      y(5,4)=y(4,5) - ym
      y(4,4)=s/18.8e3 + 1. - y(1,4) - y(4,5)
c
      y(5,6)=y(5,4)
      y(6,5)=y(5,4)
      y(5,5)=s/37.7e3 + 1. - y(4,5) - y(4,5) + ym + ym
c
      y(6,6)=-2.1*y(1,4) + s/12.6e3 - y(4,5)
      y(6,7)= .1*y(1,4)
```

```
      y(7,6)=y(6,7)
      y(6,8)=-s/75.4e3
      y(8,6)=y(6,8)
      y(6,4)=ym
      y(4,6)=ym
c
      y(7,7)=37.7e-6/s + .01 - y(6,7) - y(6,7)
      y(7,8)=y(6,7)
      y(8,7)=y(6,7)
c
      y(8,8)=s/12.6e3 - y(6,7)
c
      y(4,5)=y(5,4)
c-----------------------------------------------------------------
      call lincg(8,y,8,z,8)
c
      f = z(1,8)
c     |
      return
      end
c
c*****************************************************************
c     Function CURR
c*****************************************************************
      function curr(t)
      data t1,t2,t3,t4,t5,t6/4.167e-03,4.667e-03,8.33e-03,
     2 12.5e-03,13.0e-03,16.67e-03/
      p = t/t6
      p = aint(p)
      tp = t - t6*p
      i=1
      if(tp.ge.t1.and.tp.lt.t2)i=2
      if(tp.ge.t2.and.tp.lt.t3)i=3
      if(tp.ge.t3.and.tp.lt.t4)i=4
      if(tp.ge.t4.and.tp.lt.t5)i=5
      if(tp.ge.t5.and.tp.lt.t6)i=6
      goto(1,2,3,4,5,3),i
    1 curr=(tp**3)*13824e3
      return
    2 curr= -2000.*(tp-t2)
      return
    3 curr=0.
      return
    4 curr= -((tp-t3)**3)*13824e3
      return
    5 curr= 2000.*(tp-t5)
      return
      end
c
C  ************************************************************
C  Subroutine FHT2T
C  ================
C  Radix-2 decimation in time fast Hartley transform
C
```

```
C  Input   X          Sequence to be transformed
C          N,M        Length of sequence N = 2**M
C  Output  X          Hartley transform
C
C  Authors: D.L. Jones and H.V. Sorenson
C           Rice University, August 5, 1984
C
C  ***********************************************************
      subroutine fht2t(x,n,m)
      real x(1)
C
C-----Digit reverse counter-------------------------------
C
 100  j = 1
      n1 = n - 1
      do 104 i = 1,n1
        if (i.ge.j) goto 101
          xt = x(j)
          x(j) = x(i)
          x(i) = xt
 101    k = n/2
 102    if (k.ge.j) goto 103
          j = j - k
          k = k/2
          goto 102
 103    j = j + k
 104  continue
C
C-----Main FHT loops--------------------------------------
C
      do 10 i = 1,n,2
        xt = x(i)
        x(i) = xt + x(i+1)
        x(i+1) = xt - x(i+1)
 10   continue
C
      n2 = 1
      do 20 k = 2,m
        n4 = n2
        n2 = n4 + n4
        n1 = n2 + n2
        e = (8. * atan(1.))/n1
C
        do 30 j = 1,n,n1
          l2 = j + n2
          l3 = j + n4
          l4 = l2 + n4
          xt = x(j)
          x(j) = xt + x(l2)
          x(l2) = xt - x(l2)
          xt = x(l3)
          x(l3) = xt + x(l4)
          x(l4) = xt - x(l4)
```

```
            a = e
C
            do 40 i = 2,n4
              l1 = j + i - 1
              l2 = j - i + 1 + n2
              l3 = l1 + n2
              l4 = l2 + n2
              cc1 = cos(a)
              ss1 = sin(a)
              t1 = x(l3)*cc1 + x(l4)*ss1
              t2 = x(l3)*ss1 - x(l4)*cc1
              a = i * e
              xt = x(l1)
              x(l1) = xt + t1
              x(l3) = xt - t1
              xt = x(l2)
              x(l2) = xt + t2
              x(l4) = xt - t2
 40         continue
 30       continue
 20     continue
C
        return
        end
```